

draft November 2, 2018

Bayesian Method for Disease QTL Detection and Mapping, using a Case and Control Design and DNA Pooling

Toby Johnson¹

School of Biological Sciences, The University of Edinburgh

West Mains Road, Edinburgh, EH9 3JT

toby.johnson@ed.ac.uk

ABSTRACT

This paper describes a Bayesian statistical method for determining the genetic basis of a complex genetic trait. The method uses a sample of unrelated individuals classified into two groups, for example cases and controls. Each group is assumed to have been genotyped at a battery of marker loci using a laboratory effort efficient technique called DNA pooling. The aim is to detect and map a quantitative trait locus (QTL) that is *not* one of the typed markers. The method works by conducting an exact Bayesian analysis under a number of simplifying population genetic assumptions that are somewhat unrealistic. Despite this, the method is shown to perform acceptably on datasets simulated under a more realistic model, and furthermore is shown to outperform classical single point methods.

1. Introduction

For many traits of interest, including susceptibility to many genetic diseases, the genetic basis is complex, meaning that many genes of individually small effect (quantitative trait loci; QTLs) contribute. For detecting and mapping such QTLs, association mapping studies that use large samples of essentially unrelated individuals may have two advantages over linkage studies that use pedigrees or families: For a given sample size, association studies may have

¹Jointly affiliated to Rothamsted Research and to The University of Edinburgh

more power to detect a QTL (e.g. Risch and Merikangas 1996, Risch 2000), and they may allow the QTL to be fine mapped with greater resolution or precision (e.g. Terwilliger 1995, McPeck and Strahs 1999). One important experimental design is a genome wide scan, in which many thousands of markers covering the whole genome are typed (see e.g. Lander 1996, Risch and Merikangas 1996, Kruglyak 1999, Carlson *et al.* 2003). The aim may be to detect QTL that are not candidate genes and that have escaped detection in linkage studies. After preliminary analysis, attention may focus on relatively small chromosomal regions, each containing perhaps only one QTL. Because of nongenetic factors and the effects of other genetically distant QTLs, each focal QTL will explain only a small fraction of the variance in phenotype. If the trait is binary (such as presence or absence of a disease), the difference in QTL allele frequencies between the two trait groups will be small. The large numbers of markers required for a genome wide scan will need to have been typed in large numbers of individuals to detect such a QTL, and to infer its position, frequency, and effect on the trait.

In order to reduce the cost of such a study, an experimental strategy called DNA pooling has been proposed (e.g. Arnheim *et al.* 1985, Barcellos *et al.* 1997, Sham *et al.* 2002, Norton *et al.* 2004). Here DNA from individuals with similar phenotypes is physically mixed together into a pool before genotyping. After overheads to do with construction of pools and assay development, the cost of genotyping an entire pool at a given marker is reduced to the cost of genotyping a single individual. Thus costs may be reduced by a factor close to the number of individuals in a pool (divided by the number of experimental replicates used for each pool), when the overheads can be spread across many markers and across many disease studies.

In this paper I consider the simplest experimental design where there are two trait groups. These could have been classified by the presence or absence of binary trait such as a disease. Alternatively, if the trait is quantitative, individuals from each tail of the trait distribution could make up the two groups, for example the upper and lower 10% tails (e.g. Darvasi and Soller 1994, Bader *et al.* 2001). For simplicity I will refer throughout the paper to the two trait groups as cases and controls, and to one of the alleles at the QTL as the disease allele. I note that data collected from more than two groups can be analysed using the method developed here, by discarding or combining data from some of the groups. (An extreme example is where each pool contains two chromosomes, i.e. genotype data are available.) Such an approach is valid and may be useful, but will almost certainly not make most efficient use of the available data, since it will be based on only a marginal observation that is almost certainly not sufficient.

Compared with individual genotyping, a DNA pooling strategy incurs three types of information loss and error. At each marker only the marginal counts of the alleles present

within each pool are available, and so there is (i) no information about deviations from Hardy–Weinberg proportions within each marker within each pool (Risch and Teng 1998) and (ii) no information about phase or linkage information across markers within each pool (Johnson 2005). Further (iii), the marginal counts are only estimated from some kind of quantitative genotyping experiment (e.g. Germer *et al.* 2000, Le Hellard *et al.* 2002), rather than by counting individual genotyping experiments.

The present approach deals with (iii) by allowing a quite general class of models for errors in allele frequency estimation. It attempts to deal with (i) and (ii) by using the full likelihood given the available data. This likelihood does however assume a model that makes simplifying assumptions that are not as realistic as one would like. This may be an acceptable price to pay, because it allows all the necessary computations to be done analytically or using simple numerical algorithms. The aim is to develop a method that can be used on very large data sets, with hundreds of cases and hundreds of controls typed at hundreds of markers.

The simple model used here is a special case of the model introduced by McPeck and Strahs (1999) and studied by Morris *et al.* (2000), Zhang and Zhao (2000, 2002) and Liu *et al.* (2001) for haplotype and genotype data. In brief summary, I assume a unique mutation event (perhaps a single nucleotide polymorphism, or a deletion) generated the disease allele at the disease QTL, that there is a star shaped genealogy since that mutation, that the disease allele is absent from the control group, and that Hardy–Weinberg and linkage equilibrium apply in the control group.

Avoiding the use of more complicated algorithms such as Markov chain Monte Carlo (MCMC) means that there are no concerns about mixing and convergence, and no difficulties with computing normalising constants and Bayes factors for model testing and model comparison. When the model is correct, the Bayes factor is (in various classical senses, see O’Hagan and Forster 2004 ch.5) an optimal test statistic for detecting a QTL (see also Patterson *et al.* 2004). Therefore the present approach can be viewed as choosing an approximate model that is simple enough to allow an exact and optimal analysis. It will therefore complement alternative approaches that perform approximate or sub-optimal analyses for more realistic models.

One example of such an alternative approach is to perform a classical single point analysis, which applies a separate test to the data for each marker. Such an approach can be made essentially free of any population genetic model, meaning that no worrying assumptions are made but also that there is no efficient framework for combining analyses across many markers (e.g. to correct for multiple testing). When genotype data are available and when the QTL is *not* one of the typed markers, such single point methods are known to lack power (e.g. Risch 2000, Mott *et al.* 2000, Zollner and Pritchard 2005), and may produce inefficient

point estimates and inefficiently large region estimates for the position of the QTL (e.g. Morris *et al.* 2002, 2003).

One justification for the method developed here is that although the model is simple, it is to my knowledge the most complex model for which a Bayesian analysis has been implemented using data from DNA pools. To provide further justification and reassurance about the simplifying assumptions made, I have tested the method on data simulated under a more realistic full coalescent model. The (necessarily classical) measures of performance are encouraging in three respects. Firstly, the power to detect a QTL is substantially higher than for classical single point analysis. Secondly, point estimates for the position of the QTL derived from the present method outperform the simple procedure of choosing the map position of the marker with the most significant single point test result (the “minimum p -value method”, e.g. Kaplan and Morris 2001a,b). Thirdly, after “flattening” the posterior using a factor (derived by McPeck and Strahs 1999) that corrects for the fact that the true genealogy is not in fact star shaped, credibility intervals for the position of the QTL cover its true position with frequency equal to their nominal size. That is, they are well calibrated.

The structure of this paper is as follows. In section 2 I review the model introduced by McPeck and Strahs (1999), for which an exact Bayesian analysis can be performed using multilocus estimated allele frequency data, collected using DNA pools. In section 3 I describe in detail how the computations for such an analysis are performed. In section 4 I review a more realistic coalescent model that I have used to generate simulated data sets on which to test the current approach. In section 5 I describe the performance of the method developed in sections 2–3 on those simulated data sets. In section 6 I summarise the results and discuss how the method could be improved.

2. The Simplified Model and Prior

The main notations and abbreviations used are listed in table 1, and the conditional independencies of the variables are represented in figure 1.

I assume the data (collectively denoted $\hat{\mathbf{y}}$) consist of allele frequency estimates at L single nucleotide polymorphisms (SNPs), obtained from a single pool of n_d case chromosomes and a single pool of n_c control chromosomes. Let m_i be the known map position of the i -th SNP. Let the alleles at each SNP be arbitrarily labelled 0 and 1, with $\hat{y}_{d,i}(1) \equiv n_d - \hat{y}_{d,i}(0)$ the estimated count of the 1 allele at the i -th SNP in the cases, and $\hat{y}_{c,i}(1) \equiv n_c - \hat{y}_{c,i}(0)$ the estimated count of the 1 allele at the i -th SNP in the controls. When there is no ambiguity, \hat{y} will mean the estimated count of the 1 allele at some SNP in some pool that is to be

inferred from the context. (This can easily be generalised to let $\hat{y}_{d,i}$ be arbitrary vector valued information about the counts of the two alleles at the i -th SNP in the cases, etc.) The method may be generalised to allow more than two alleles at each marker.

Let $y_{d,i}(1)$ and $y_{c,i}(1)$ be the true counts of the 1 allele at the i -th SNP in the cases and in the controls respectively. I assume that an error model $\Pr(\hat{y}_{d,i}, \hat{y}_{c,i} | y_{d,i}, y_{c,i})$ has been chosen and parameterised, for example from a calibration data set consisting of pairs (\hat{y}, y) that were obtained from a given set of individuals by genotyping them as a pool and by genotyping them individually. Note that the error model cannot be factorised unless we assume that the errors in the case and control pools are unconditionally independent. However, we may believe that the data were obtained using assays that vary in precision across SNPs. Letting e_i indicate the unknown precision of the assay used for the i -th SNP, we could model these beliefs as

$$\Pr(\hat{y}_{d,i}, \hat{y}_{c,i} | y_{d,i}, y_{c,i}) = \sum_{e_i} \Pr(\hat{y}_{d,i} | y_{d,i}, e_i) \Pr(\hat{y}_{c,i} | y_{c,i}, e_i) \Pr(e_i), \quad (1)$$

that is, the error distribution is modelled as a mixture distribution where each component of the mixture factorises. In the following, reasonable flexibility in the nature of this error model is allowed: the errors must be independent across SNPs but they need not be independent across pools and they do not need to be identically distributed across SNPs. A example error model is given in section 4.

Let the unknown map position of the disease QTL relative to the leftmost marker SNP be μ ; often this will be the variable of main interest. I allow any prior $\Pr(\mu)$; obvious choices would be a uniform density on physical distance, or one based on known gene density (see e.g. Rannala and Reeve 2001). I assume a unique mutation event generated the disease allele at the disease QTL, so some number of haplotypes (x_μ) in the case pool carry the disease allele and are identical by descent (i.b.d.) at this position. I assume $x_\mu \sim \text{Bin}(n_d, \rho)$ for a rate ρ , and since ρ itself is uncertain I assume a beta prior with parameter $R = (R_1, R_0)$, so the prior mean is $R_1/(R_0 + R_1)$. Specifying $(R_1, R_0) = (1, 1)$ specifies a flat prior on $[0, 1]$ for ρ . I assume that the disease allele is absent from the control pool. The adequacy of this approximation, and ways in which it could be relaxed, are taken up in the discussion in section 6.

Each disease allele is embedded in a block of i.b.d. haplotype, the “ancestral haplotype”, with breakpoints at distances d_L and d_R to the left and right of the position of the QTL. I assume a star shaped genealogy for the disease allele, so that d_L and d_R for all blocks of ancestral haplotype are conditionally independent and identically distributed (i.i.d.) from an exponential distribution with mean $1/\tau$ Morgans, where τ is the age of the disease allele in generations and distances are measured in Morgans (McPeck and Strahs 1999, see also Morris *et al.* 2000, Zhang and Zhao 2000, 2002, Liu *et al.* 2001). (The left and right breakpoints

are the positions of the nearest crossovers in τ meioses where crossovers occur as a Poisson process with rate 1.) I allow any prior $\Pr(\tau)$; lognormal and gamma are reasonable choices. Specifying an exponential prior with sufficiently small parameter T (so the prior mean $1/T$ is sufficiently large) specifies a prior that is effectively flat over the region where the likelihood is non-negligible. This has the effect of making the posterior model probability or Bayes factor proportional to T . A crucial variable in the analysis is x_i , the number of chromosomes in the case pool that carry the i.b.d. haplotype at the i -th SNP. The assumptions above specify a distribution for the x_i . A key feature of the present method is that the x_i are not independent across SNPs, in contrast to what is assumed in composite likelihood methods (e.g. Terwilliger 1995, Xiong and Guo 1997, Collins and Morton 1998, Maniatis *et al.* 2004, 2005).

All other non-i.b.d haplotype is called heterogenous “non-ancestral haplotype”. The allele present in non-ancestral haplotype is assumed conditionally independent across chromosomes within SNPs, and across SNPs within chromosomes, with $\pi_i(1)$ the probability of a 1 allele at the i -th SNP and $\pi_i(0) \equiv 1 - \pi_i(1)$. (This is equivalent to assuming Hardy–Weinberg and linkage equilibrium in blocks of non-ancestral chromosome.) This assumption is a very bad one when haplotype or genotype data are available (Liu *et al.* 2001, Morris *et al.* 2002, Li and Stephens 2003), but when only multilocus allele frequency data are available it may be more innocuous; this assumption leads to a massive simplification in the likelihood. I assume an independent beta prior for each $\pi_i(1)$, with parameter $P_i = (P_{i,1}, P_{i,0})$, so the prior mean is $P_{i,1}/(P_{i,0} + P_{i,1})$. The method should be robust to misspecification of P_i as long as both elements are much smaller than n_c .

The allele present on the ancestral haplotype at the position of the i -th SNP, a_i , is assumed to be a single draw from the same distribution as for a block of nonancestral chromosome. That is, each a_i is an independent Bernoulli variable with parameter $\pi_i(1)$.

3. Analysis

3.1. Overview

The purpose of the analysis is to compute the posterior distribution for quantities of interest. Here I focus on computing the Bayes factor in favour of a model in which a QTL is present, versus a model with no QTL. This Bayes factor allows the posterior model probabilities to be computed for any prior on the two models. I also compute the posteriors for μ , τ and ρ , given that a QTL is present, marginalising all other variables.

The model has a hierarchical structure as shown in figure 1. Note that the joint distri-

bution of the x_i depends on μ , τ and ρ , but that the probability of the data at the i -th SNP only depends on x_i and other variables π_i and a_i for which the prior is independent across SNPs. The first step of the analysis, in section 3.2, is to perform an independent calculation for each SNP that integrates out π_i and a_i conditional on x_i . The second step of the analysis, in section 3.3, is to integrate out all the x_i and x_μ conditional on μ , τ and ρ . This gives the posterior density for these three variables. The final step, in section 3.4, is to compute the marginal posteriors for each of μ , τ and ρ , and the normalising constant or probability of the data given models with and without a QTL.

3.2. Calculations for the i -th SNP

Note that all probabilities in this section are conditional on x_i , the number of chromosomes in the case pool carrying the ancestral i.b.d. chromosome. At the i -th SNP let $y_{d,i}(1) \equiv n_d - y_{d,i}(0)$ be the (unknown) actual count of the 1 allele in cases, and $y_{c,i}(1) \equiv n_c - y_{c,i}(0)$ be the actual estimated count of the 1 allele in controls. Let $y_{d,i} = (y_{d,i}(1), y_{d,i}(0))$ and a similar notation apply for controls. Under the modelling assumptions we have

$$\Pr(y_{d,i}|x_i, a_i, \pi_i) = \text{Bin}(y_{d,i}(a_i) - x_i, n_d - x_i, \pi_i(a_i)) \quad (2)$$

$$\Pr(y_{c,i}|\pi_i) = \text{Bin}(y_{d,i}(1), n_c, \pi_i(1)) \quad (3)$$

where $\text{Bin}(x, n, p)$ is the probability of observing x successes in n independent trials with success probability p (and understood to be zero unless $0 \leq x \leq n$). For a more detailed motivation of (2) and (3) see Johnson (2005 appendix A)

Then the probability of the observed data can be written

$$\Pr(\hat{y}_{d,i}, \hat{y}_{c,i}|x_i, a_i, \pi_i) = \sum_{y_{d,i}} \sum_{y_{c,i}} \Pr(\hat{y}_{d,i}, \hat{y}_{c,i}|y_{d,i}, y_{c,i}) \Pr(y_{d,i}|x_i, a_i, \pi_i) \Pr(y_{c,i}|\pi_i). \quad (4)$$

We can simplify at this stage by writing down the distribution marginal to a_i and π_i and moving the respective sum and integral as far inside the expression as possible, to get

$$\begin{aligned} \Pr(\hat{y}_{d,i}, \hat{y}_{c,i}|x_i) &= \sum_{y_{d,i}} \sum_{y_{c,i}} \left(\Pr(\hat{y}_{d,i}, \hat{y}_{c,i}|y_{d,i}, y_{c,i}) \right. \\ &\quad \left. \int \sum_{a_i} (\Pr(y_{d,i}|x_i, a_i, \pi_i) \Pr(a_i|\pi_i)) \Pr(y_{c,i}|\pi_i) \Pr(\pi_i) d\pi_i \right). \end{aligned} \quad (5)$$

The innermost sum over a_i can be rewritten

$$\Pr(y_{d,i}|x_i, \pi_i) = \sum_{a_i} \Pr(y_{d,i}|x_i, a_i, \pi_i) \Pr(a_i|\pi_i) \quad (6)$$

$$= \sum_{a_i} \left(\text{Bin}(y_{d,i}(a_i) - x_i + 1, n_d - x_i + 1, \pi_i(a_i)) \right. \\ \left. \times \binom{n_d - x_i}{y_{d,i}(a_i) - x_i} / \binom{n_d - x_i + 1}{y_{d,i}(a_i) - x_i + 1} \right) \quad (7)$$

$$= \sum_{a_i} \left(\text{Bin}(y_{d,i}(a_i) - x_i + 1, n_d - x_i + 1, \pi_i(a_i)) \right. \\ \left. \times \frac{y_{d,i}(a_i) - x_i + 1}{n_d - x_i + 1} \right). \quad (8)$$

This allows the integral over π_i to be computed analytically when (as assumed above) the prior $\Pr(\pi_i(a_i))$ is a beta distribution with parameter $(P_{i,a_i}, P_{i,1-a_i})$

$$\Pr(y_{d,i}, y_{c,i}|x_i) = \int \Pr(y_{d,i}|x_i, \pi_i) \Pr(y_{c,i}|\pi_i) \Pr(\pi_i) d\pi_i \quad (9)$$

$$= \sum_{a_i} \left(\frac{(n_d - x_i + 1)! \Gamma(n_c + P_{i,0} + P_{i,1})}{\Gamma(n_d - x_i + 1 + n_c + P_{i,0} + P_{i,1})} \right. \\ \times \frac{\Gamma(y_{d,i}(a_i) - x_i + 1 + y_{c,i}(a_i) + P_{i,a_i})}{(y_{d,i}(a_i) - x_i + 1)! \Gamma(y_{c,i}(a_i) + P_{i,a_i})} \\ \times \frac{\Gamma(y_{d,i}(1 - a_i) + y_{c,i}(1 - a_i) + P_{i,1-a_i})}{y_{d,i}(1 - a_i)! \Gamma(y_{c,i}(1 - a_i) + P_{i,1-a_i})} \\ \left. \times \frac{y_{d,i}(a_i) - x_i + 1}{n_d - x_i + 1} \right) \quad (10)$$

Thus the probability of the observed data reduces to

$$\Pr(\hat{y}_{d,i}, \hat{y}_{c,i}|x_i) = \sum_{y_{d,i}} \sum_{y_{c,i}} \Pr(\hat{y}_{d,i}, \hat{y}_{c,i}|y_{d,i}, y_{c,i}) \Pr(y_{d,i}, y_{c,i}|x_i) \quad (11)$$

where the first term in the summand is the error model and the second term is given by (10).

Because $\hat{y}_{d,i}$ and $\hat{y}_{c,i}$ are fixed and a_i and π_i have been integrated out, values of (11) for each x_i can be precomputed and stored in a small lookup table of size $(n_d + 1)$. It is therefore feasible to use a complicated and hopefully realistic error distribution, as discussed above. For many error models, computation can be speeded up without loss of accuracy by judicious reduction of the range of the summation in (11).

3.3. Hidden Markov Model for x_μ and the x_i

Throughout this section, all probabilities are conditional on given values of μ , τ and ρ but to make a clearer exposition this is suppressed in the notation.

Assume for clarity of exposition that μ is a position within the battery of marker SNPs. Let $\lceil \mu \rceil = \min \{i : m_i \geq \mu\}$ and $\lfloor \mu \rfloor = \max \{i : m_i < \mu\}$ denote the indices of the SNPs to the right and left of the QTL. The algorithm works with obvious modifications when μ is a position outside the battery of marker SNPs.

Under the modelling assumptions, as we move away from the position of the disease locus, the number of chromosomes containing i.b.d. ancestral chromosome, x_i , is Markovian. The *transition probabilities* of a (nonstationary and inhomogenous) hidden Markov model (HMM; see e.g. Durbin *et al.* 1998 ch.3), for marker SNPs to the right of μ (i.e. $\lceil \mu \rceil \leq i$), are

$$\Pr(x_{i+1}|x_i) = \text{Bin}(x_{i+1}, x_i, \exp(-\tau \times (m_{i+1} - m_i))) \quad (12)$$

Similar equations hold for for marker SNPs to the left of μ , and for $\Pr(x_i|x_\mu)$. The *emission probabilities* of the HMM are given by (11). There is an important difference between this HMM and the HMMs of McPeck and Strahs (1999), Morris *et al.* (2000), Zhang and Zhao (2000, 2002) and Liu *et al.* (2001). Those authors modelled the observed haplotypes or genotypes as a set of conditionally independent HMMs, conditional on (in the present notation) (a_1, \dots, a_L) , (π_1, \dots, π_L) as well as μ , τ and ρ . Thus they had to use expensive numerical algorithms (optimisation or MCMC) on the high dimensional space of variables on which the HMMs were conditioned. Here I am able to model all the data as a *single* HMM conditional on only μ , τ and ρ . I am thus able to integrate out the high dimensional (a_1, \dots, a_L) and (π_1, \dots, π_L) using an efficient numerical algorithm and am left with only a low dimensional space (the space for (μ, τ, ρ)) on which I will need to use an expensive numerical algorithm.

We can use the backwards propagation algorithm for HMMs to sum over the hidden states (x_1, \dots, x_L) (see e.g. Durbin *et al.* 1998 ch.3, Liu 2001 pp.28–31). Readers familiar with HMMs may wish to skip the rest of this section.

Define the *backwards variables* for SNPs at positions to the right of the QTL

$$b(x_i) := \Pr(\hat{y}_{d,i+1}, \hat{y}_{c,i+1}, \dots, \hat{y}_{d,L}, \hat{y}_{c,L} | x_i) \quad (13)$$

and for SNPs at positions to the left of the QTL

$$b'(x_i) := \Pr(\hat{y}_{d,1}, \hat{y}_{c,1}, \dots, \hat{y}_{d,i-1}, \hat{y}_{c,i-1} | x_i) \quad (14)$$

Here backwards is relative to the direction in which the hidden process is Markovian. Equation (14) should not be confused with a forwards variable, which are not used in this computation. Note also that the backwards variables are functions of which SNP (i) and the value of that x_i at that SNP, but that I have adopted a more streamlined notation that I hope is unambiguous.

The backwards variables have the obvious interpretation when the arguments run out of range, that

$$b(x_L) := \Pr(\text{nothing}|x_L) = 1 \quad (15)$$

$$b'(x_1) := \Pr(\text{nothing}|x_1) = 1 \quad (16)$$

Using (16) to *initialise* the backwards variables at $i = L$, we then proceed to *propagate* leftwards along the chromosomes for each $i = L - 1, \dots, \lceil \mu \rceil$ in turn, compute the backwards variables for every (x_i) using

$$b(x_i) = \sum_{x_{i+1}} \Pr(x_{i+1}|x_i) \Pr(\hat{y}_{d,i+1}, \hat{y}_{c,i+1}|x_{i+1}) b(x_{i+1}) \quad (17)$$

and then *terminate* the algorithm by computing

$$\Pr(\hat{y}_{d,\lceil \mu \rceil}, \hat{y}_{c,\lceil \mu \rceil}, \dots, \hat{y}_{d,L}, \hat{y}_{c,L}|x_\mu) = \sum_{x_{\lceil \mu \rceil}} \Pr(x_{\lceil \mu \rceil}|x_\mu) \Pr(\hat{y}_{d,\lceil \mu \rceil}, \hat{y}_{c,\lceil \mu \rceil}|x_{\lceil \mu \rceil}) b(x_{\lceil \mu \rceil}) \quad (18)$$

for every x_μ .

Likewise, using (16) to initialise the b' backwards variables at $i = 1$ we can propagate rightwards along the chromosomes (backwards in the sense that time or space is usually considered in HMMs) for $i = 2, \dots, \lfloor \mu \rfloor$ and terminating in a symmetric manner to compute $\Pr(\hat{y}_{d,1}, \hat{y}_{c,1}, \dots, \hat{y}_{d,\lfloor \mu \rfloor}, \hat{y}_{c,\lfloor \mu \rfloor}|x_\mu)$.

We then obtain the probability of all the data by computing

$$\begin{aligned} \Pr(\hat{\mathbf{y}}) &= \Pr(\hat{y}_{d,1}, \hat{y}_{c,1}, \dots, \hat{y}_{d,L}, \hat{y}_{c,L}) \\ &= \sum_{x_\mu} \left(\text{Bin}(x_\mu, n_d, \rho) \Pr(\hat{y}_{d,1}, \hat{y}_{c,1}, \dots, \hat{y}_{d,\lfloor \mu \rfloor}, \hat{y}_{c,\lfloor \mu \rfloor}|x_\mu) \right. \\ &\quad \left. \Pr(\hat{y}_{d,\lceil \mu \rceil}, \hat{y}_{c,\lceil \mu \rceil}, \dots, \hat{y}_{d,L}, \hat{y}_{c,L}|x_\mu) \right) \end{aligned} \quad (19)$$

Restoring the conditioning that has been implicit throughout this section, (19) is $\Pr(\hat{\mathbf{y}}|\mu, \tau, \rho)$, the probability of all the data conditional on (μ, τ, ρ) and marginal to (a_1, \dots, a_L) and (π_1, \dots, π_L) .

3.4. Marginal Posteriors for μ , τ and ρ and Model Probabilities

The posterior for μ , τ and ρ , up to a normalising constant, is obtained simply by multiplying (19) by the relevant priors.

$$\Pr(\hat{\mathbf{y}}, \mu, \tau, \rho) = \Pr(\hat{\mathbf{y}}|\mu, \tau, \rho) \Pr(\mu) \Pr(\tau) B(\rho, R_1, R_0) \quad (20)$$

so

$$\Pr(\mu, \tau, \rho|\hat{\mathbf{y}}) = \Pr(\hat{\mathbf{y}}|\mu, \tau, \rho) \Pr(\mu) \Pr(\tau) B(\rho, R_1, R_0) \frac{1}{\Pr(\hat{\mathbf{y}})} . \quad (21)$$

Summarising this posterior is not entirely trivial for large data sets, because computing the posterior at any given point (μ, τ, ρ) using the propagation algorithm of section 3.3 takes on the order of $L n_d^2$ operations (and all addition has to be done in log-space, see e.g. Durbin *et al.* (1998 p.77–78)), so we cannot rely on being able to make an arbitrarily large number of such computations.

I use Cartesian product quadrature (CPQ; see e.g. O’Hagan and Forster 2004 **9.43–9.44**) to compute marginal posteriors for each of μ , τ or ρ , and the normalising constant or marginal likelihood $\Pr(\hat{\mathbf{y}})$ assuming there is a disease QTL. CPQ makes the approximation

$$\begin{aligned} \Pr(\hat{\mathbf{y}}) &= \int \int \int \Pr(\hat{\mathbf{y}}, \mu, \tau, \rho) d\mu d\tau d\rho \\ &\simeq \sum_j \sum_k \sum_\ell w_j^{(\mu)} w_k^{(\tau)} w_\ell^{(\rho)} \Pr(\hat{\mathbf{y}}, \mu_j, \tau_k, \rho_\ell) \end{aligned} \quad (22)$$

where e.g. j indexes a set of *design points* $\{\mu_1, \mu_2, \dots\}$, and $w_j^{(\mu)}$ is a *weight* associated with the j -th design point. (A quantity proportional to) the marginal posterior for any variable μ , τ or ρ is obtained by omitting the respective sum from (22). When computed using priors describing our beliefs about these variables given that there is a QTL in the region of interest, the quantity in (22) will be called $\Pr(\hat{\mathbf{y}}|\text{QTL})$.

The choice of design points and weights depends on the region of interest and the prior, and the quadrature rule to be used. For example, all calculations in section 5 the region of interest is $\mu \in (0, 1)$, measured in Mb or cM. With a uniform prior for μ , exponential prior for T with $T = 1/1000$, and flat beta prior for ρ with $R_1 = R_0 = 1$, I used 100 design points for each variable as follows:

$$\begin{aligned} \mu_j &= (j + 1/2) / 100, & w_j^{(\mu)} &= 0.01, & j &= 0, 1, \dots, 99 \\ \tau_k &= \exp(k/11), & w_k^{(\tau)} &= \exp(k/11)/11, & k &= 0, 1, \dots, 99 \\ \rho_\ell &= (\ell + 1/2) / 100, & w_\ell^{(\rho)} &= 0.01, & \ell &= 0, 1, \dots, 99 \end{aligned} \quad (23)$$

Here the quadrature rule is very simple and corresponds approximately to the trapezoid rule or two point Newton–Cotes rule.

A simple model with no QTL is to assume there are no blocks of i.b.d. haplotype, $x_i = 0$ for all i . This corresponds to a degenerate prior at $\rho = 0$ (or the limits $\mu \rightarrow \pm\infty$ or $\tau \rightarrow \infty$). The probability of the data under this model, $\Pr(\hat{\mathbf{y}}|\text{no QTL})$, is easily computed directly from (11). The Bayes factor (BF) in favour of the model with a QTL is then

$$\text{BF} = \frac{\Pr(\text{QTL}|\hat{\mathbf{y}})}{\Pr(\text{no QTL}|\hat{\mathbf{y}})} \bigg/ \frac{\Pr(\text{QTL})}{\Pr(\text{no QTL})} = \frac{\Pr(\hat{\mathbf{y}}|\text{QTL})}{\Pr(\hat{\mathbf{y}}|\text{no QTL})}. \quad (24)$$

In addition to its Bayesian interpretation, the BF (or any isotonic transformation thereof) has good properties, from a classical frequentist perspective, as a test statistic to test the null model with no QTL against the alternative with a QTL (O’Hagan and Forster 2004 ch.5, Patterson *et al.* 2004). Tests based on the BF are admissible, which means that no other test has greater power for all (μ, τ, ρ) . There may be other tests that have greater power for some (μ, τ, ρ) , and are therefore also admissible, but it is “unusual and strange” to find an admissible test that is not based on the BF computed using *some* prior. Furthermore, (up to isomorphism) the BF uniquely maximises average power, when the averaging is done with respect to the prior for (μ, τ, ρ) used to compute the BF. Of course, this theory only applies when the model is correct, but we might hope that the most powerful test for an approximate model would be approximately most powerful for a more realistic model. The BF is a sensible way to combine information across many markers to produce a single test, and thus avoids (or overcomes) the problematic need to correct for multiple testing (Patterson *et al.* 2004).

I have also implemented a Markov chain Monte Carlo (MCMC; see e.g. Gilks *et al.* 1996, Liu 2001) sampler, which uses the Metropolis–Hastings algorithm to sample from the posterior density for (μ, τ, ρ) . A proposal distribution that seems to work reasonably well is to update a single variable, chosen at random with equal probability, using the following:

$$\begin{aligned} \mu' &\sim \text{N}(\mu, (0.1(m_L - m_1))^2) \\ t' &\sim \text{G}(10, t/10) \\ r' &\sim \text{B}(5r, 5(1 - r)) \end{aligned} \quad (25)$$

Kernel based methods (see e.g. Silverman 1986) can then be used to estimate marginal posteriors for each of the variables, and these seemed similar to the marginal posteriors computed using CPQ in the cases I examined. However, standard numerical methods to estimate the model probability $\Pr(\hat{\mathbf{y}})$ from the MCMC output (see e.g. O’Hagan and Forster 2004 **10.46**) converged very slowly and did not seem reliable.

In addition to the ease and reliability with which the normalising constant or BF can be computed, CPQ offers substantial advantages over alternatives such as MCMC in low

dimensional situations such as this one. There are no concerns about burnin or mixing. CPQ makes efficient use of the evaluation of the posterior density at each design point. We can investigate sensitivity to prior specification afterwards without redoing much of the computation.

In this particular situation CPQ offers an additional advantage, that by traversing the design points in a particular order many of the backwards variables computed in the propagation algorithm of section 3.3 it be stored and reused, and thus a CPQ algorithm with n design points runs much faster than a MCMC algorithm with n samples. The details are as follows: The posterior can be computed on all points on a three dimensional lattice most efficiently by traversing the lattice with different values of τ in the outermost loop, different values of μ in the middle loop, and different values of ρ in the innermost loop. This is because each time ρ changes but μ and τ do not then only (19) has to be recomputed. Each time μ changes but τ does not then (18) always has to be recomputed, and if the old and new values of μ are separated by one or more typed SNPs then one or more columns of backwards variables also have to be recomputed. If μ always increases then the b are all computed first and then as the lattice is traversed extra columns of b' are computed and columns of b are simply discarded. Changing τ means that the transition probabilities (12) change and everything has to be recomputed. The run time of the whole algorithm (propagation and CPQ) scales quadratically in n_d and linearly in $L + d_\mu$ where d_μ is the number of design points used for μ . If a small map region is found to be interesting additional design points can be added later at moderate cost.

The disadvantages of CPQ are that we learn little about the posterior until calculations have been completed for all the design points, we may belatedly discover that our choice of design points was not a good one, that MCMC *may* be more sensitive to very narrow spikes containing substantial probability mass (these will be missed if they fall inbetween the design points) and that CPQ will not scale well to higher dimensional spaces which we might need to study if we elaborated the model.

4. Coalescent Simulation Model and Error Model

In this section I describe a more realistic model that was used to simulate datasets on which to test the method described above in sections 2–3. I also describe a specific model for errors in allele frequency estimation. Each simulated dataset was generated as follows.

First I used the `mksamples` program of Hudson (2002) to simulate a sample of 20,000 1Mb long regions, assuming the standard neutral coalescent model with population recom-

bination rate $4N_e c = 400$ ($N_e = 10,000$ assuming 1cM/Mb), and assuming the infinite sites mutation model with population mutation rate $4N_e \mu = 10$. (This is an unrealistically low mutation rate, the idea is to simulate some of the SNPs in the region rather than all of them.) Chromosomes were paired at random to generate a sample of 10,000 individuals.

One SNP with a minor allele frequency between 10% and 20% was chosen as the disease QTL. The disease status of each individual was simulated assuming multiplicative risks, so that $\gamma_{01}/\gamma_{00} = \gamma_{11}/\gamma_{01} = g$. Here γ_G is the penetrance (probability of having the disease) given genotype G at the disease QTL, with 1 the minor allele. The parameter g is called the allelic or genotype relative risk (see e.g. Risch and Merikangas 1996). Simulations for this paper used values of $g = 4$ and $g = 1$. The penetrance of the wild type homozygote, γ_{00} , was set so that the marginal probability of having the disease was 0.02. (Thus the number of case chromosomes n_d was random with expectation $0.02 \times 10,000 \times 2 = 400$.) Data from all $n_d/2$ case individuals, and an equal number $n_c/2$ of randomly chosen control individuals, were used to make up the two pools.

Excluding the disease QTL, all simulated SNPs with a minor allele frequency greater than 0.05 in the $n_c/2$ individuals in the control pool were analysed, so the number of SNPs L was also random. The estimated allele frequencies at each SNP and for each pool were either assumed to be known exactly, or assuming that allele frequencies were estimated using the lag between kinetic PCR growth curves (Germer *et al.* 2000), using

$$\hat{y} = \frac{1}{1 + 2\Delta\hat{C}_t} \times n. \quad (26)$$

Here \hat{y} is shorthand for the estimated count of the 1 allele, n is the number of chromosomes in the pool, $\Delta\hat{C}_t = \hat{C}_t(1) - \hat{C}_t(0)$, and $\hat{C}_t(a)$ is the number of PCR cycles before the amount of PCR product for allele a exceeds some threshold level (Germer *et al.* 2000). The model for $\Pr(\hat{y}|y, e)$ is then as follows: Define the true lag $\Delta C_t = \log_2((n - y)/y)$, which is the lag that would give the correct frequency when (26) was used. I assume that the observed lag $\Delta\hat{C}_t$ averaged across r experiments is normally distributed with mean ΔC_t and variance σ^2/r , where σ^2 is the variance in lags across replicate experiments.

Using the Jacobian

$$\frac{d\hat{y}}{d(\Delta\hat{C}_t)} = \ln(2)\hat{y}(n - \hat{y})\frac{1}{n} \quad (27)$$

we can write down the error model in the form required in (4) for the analysis,

$$\Pr(\hat{y}|y, n, \sigma^2, r) = \frac{n}{\ln(2)\hat{y}(n - \hat{y})} \frac{1}{\sqrt{2\pi\sigma^2/r}} \exp\left(-\frac{\left(\ln\left(\frac{(n-y)\hat{y}}{y(n-\hat{y})}\right)\right)^2}{2\ln(2)^2\sigma^2/r}\right). \quad (28)$$

5. Testing the Method

All measurements of the performance of the Bayesian method described in sections 2–3 are based on analyses of datasets simulated under a more realistic model, as described in section 4. Results are reported for two situations, either where the allele frequencies in each pool are known exactly, or where there are errors in allele frequency estimation using (28) and assuming that n , $r = 2$ replicates and $\sigma = 0.2$ PCR cycles are all known. This magnitude of error is comparable to those reported by Germer *et al.* (2000) and Shiffman *et al.* (2004). Using (27) we can say that these parameter values correspond to a “typical” error in allele frequency estimate \hat{y}/n of about $y/n(1 - y/n) \ln(2)\sigma/\sqrt{2} \simeq y/n(1 - y/n)0.098$ or, for intermediate allele frequencies, about 2.5%.

For each situation, allele frequencies known either exactly or estimated with errors, I analysed 500 datasets simulated assuming there was a QTL with a genotype relative risk $g = 4$, and 500 datasets simulated assuming a null model with no QTL ($g = 1$, so the penetrances $\gamma_{00} = \gamma_{01} = \gamma_{11} = 0.02$ are all equal). In these simulations, the median number of case or control individuals, $n_d/2 = n_c/2$, was 200 (interquartile range 191–209, range 154–248). The median number of SNPs, L , was 28 (interquartile range 24–32, range 12–51). These simulations assumed relative risks that are higher, and correspondingly sample sizes that are smaller than may be realistic for many studies of QTLs influencing complex genetic diseases. This reflects the need to analyse a reasonably large number of simulated datasets with the computing resources currently available to me. The mean time to run an analysis on a simulated dataset, using CPQ with the design (23) which requires evaluating the posterior at 10^6 points on a $100 \times 100 \times 100$ lattice, was about 36 minutes on a 2.4GHz Intel® Xeon™ processor (totalling about 50 processor days for all the simulated datasets).

The inferences from the Bayesian method described here are compared against simple but widely used classical single point analyses. When allele frequencies in each pool are known exactly, a chi squared test can be used on the counts of the two alleles in the two pools (see e.g. Clayton 2001), at each marker SNP separately. Visscher and Le Hellard (2003) consider how to perform an equivalent test when the errors in allele frequency estimates are Gaussian. The relatively small Gaussian errors in $\Delta\hat{C}_t$ simulated here will produce errors in allele frequency estimates that are approximately Gaussian (to the extent that (26) is linear, and in fact are underdispersed relative to a Gaussian in the direction of extreme allele frequencies). Visscher and Le Hellard (2003) show that a “shrunk” test statistic is approximately distributed as $\chi^2_{(1)}$. This shrunk statistic is equal to the ordinary χ^2 statistic computed using a point estimate of the counts, times a factor $2V_s/(2V_s + V_e)$ where V_s is the estimated sampling variance of the allele frequency due to sampling a finite number of cases and controls, under the null hypothesis of equal allele frequency in cases and controls,

and V_e is the variance of the allele frequency in either pool due to experimental error. Using (27), for the simulations performed here this shrinking factor is (approximately, for small σ)

$$\frac{2}{2 + (n_d + n_c)\hat{p}(1 - \hat{p}) \ln(2)^2 \sigma^2 / r} . \quad (29)$$

where \hat{p} is the allele frequency estimated under the null hypothesis, i.e. by pooling the case and control pools.

The most widely considered statistics from a classical single point analysis are as follows: Let p_{\min} be the smallest p -value of the L (shrunk) chi squared tests applied to a given dataset, and let $\hat{\mu}_{\min p}$ be the map position of the marker with the smallest p -value.

It is worth emphasising that all the tests described in the following sections concern the classical sense performance of statistics computed from the Bayesian analysis. Strictly, the Bayesian sense performance can only be tested by conducting a Bayesian analysis assuming a more realistic model (or prior).

5.1. Power to Detect a QTL

In this section I compare the power of tests to detect a QTL. I consider two different test statistics, and different methods of determining critical regions. The first test statistic is $2 \ln \text{BF}$, twice the logarithm of the Bayes factor (24). The second test statistic is $p_{\min} \times L$. Multiplying the smallest single point p -value by L achieves a simple Bonferonni correction for multiple testing that makes the critical region independent of L . Critical regions were determined either analytically (by arbitrary or approximate methods), or empirically (from analyses of datasets simulated under the null model). I report the performance of tests with nominal sizes of $\alpha = 0.05$ and $\alpha = 0.01$; a more general comparison is made in figures 2 and 3. For each test, the true size was estimated using 500 simulations under the null model with genotype relative risk $g = 1$, i.e. where risk is independent of genotype at the QTL. The power against an alternative with $g = 4$ was estimated using 500 simulations. For each test I report the estimated size and power, along with exact 95% binomial confidence intervals for their values.

From a Bayesian perspective, $2 \ln \text{BF} > 0$ indicates evidence in favour of the model with a QTL over the model with no QTL. As tables 2 and 3 show, the test with this critical region has small size and reasonable power. However, much more simulation work, for different models and combinations of parameters, is required to establish the generality of this result. Also, at least from a classical perspective it is desirable to be able to choose a critical region according to the size (or perhaps power) that is desired.

An arbitrary critical region is $2 \ln \text{BF} > 2 \ln (\frac{1-\alpha}{\alpha})$. I say arbitrary because this in fact guarantees nothing about the classical sense error rate, but does bound the Bayesian sense error rate: The posterior probability that there is no QTL is less than α , $\Pr(\text{no QTL}|\hat{y}) < \alpha$, when the model, the prior $\Pr(\text{QTL}) = \Pr(\text{no QTL})$, and the prior for (μ, τ, ρ) are correctly specified. It can be seen from tables 2 and 3 that these arbitrary critical regions give tests with true sizes that are smaller than α . Such tests are therefore conservative. Causes may include the simplified model used to compute the BF, the dependence of the BF on the prior specification T , and the fact that the critical region bounds the Bayesian sense error rate rather than controls the classical sense error rate. The use of these arbitrary critical regions $2 \ln \text{BF} > 2 \ln (\frac{1-\alpha}{\alpha})$ entails a loss of power due to the actual size of the test being smaller than intended, so a better method for determining a critical region is desirable.

Assuming goodness of the $\chi^2_{(1)}$ approximation, with the shrinking factor (29), and using simple Bonferonni correction, suggests an approximate critical region $p_{\min} \times L < \alpha$. These tests have true sizes equal to or slightly smaller than their nominal sizes, which is expected because the Bonferonni correction is conservative. This effect is expected to increase in severity as the marker density increases, because there will be a greater number of more positively correlated tests.

Although these respectively arbitrary and approximate methods for determining critical regions are not terribly accurate, and cannot be recommended, it is worth noting that there is no clear difference in power between the two test statistics, for tests with the same nominal size. Since the test based on $2 \ln \text{BF}$ is more conservative, it might reasonably be preferred.

It is not very meaningful to compare the power of tests with different sizes. Therefore I used simulations to estimate exact critical regions, so that the power of different tests with true size α could be compared. For these tests, the estimated size is exactly equal to the nominal size, because the same set of simulations are used to compute both values. Although the critical region for $\alpha = 0.01$ is unlikely to be well estimated using only 500 simulations, by a simple symmetry argument this procedure still allows a fair comparison across the different test statistics. In every case the test based on $2 \ln \text{BF}$ is substantially more powerful than the test based on $p_{\min} \times L$.

By combining simulations in which there is not and is a QTL, we can view test statistics as *classifiers*, and ask how well they discriminate between the two cases. The receiver operating characteristics (ROC) for the two statistics are compared in figures 2 and 3. The ROC curves are equivalent to plotting estimated power (= sensitivity) against size of test (= $1 - \text{specificity}$) for all possible tests (in fact, only all tests with non-disjoint critical regions). When viewed in this way, it can be seen that the BF based statistic is uniformly equal to or superior to the minimum p -value based statistic. The advantage of the BF is

greater when there are errors in allele frequency estimation. This may be because, when the dataset is less informative, it may be more important to have a model based way to combine information across SNPs.

For comparison, I have also plotted the ROC curves for a test statistic derived from the nonparametric likelihood approach that I have described previously (Johnson 2005). This nonparametric likelihood ratio (NLR) statistic is defined in the same way as the BF (24), using the same value for $\Pr(\hat{\mathbf{y}}|\text{no QTL})$, but makes the approximation

$$\Pr(\hat{\mathbf{y}}|\text{QTL}) \simeq \prod_{i=1}^L \Pr(\hat{y}_{d,i}, \hat{y}_{c,i} | x_i^*) \quad (30)$$

where $(x_1^*, x_2^*, \dots, x_L^*)$ is the set of hidden states in the HMM that maximise the probability (30) under an order restriction that they are either a weakly increasing sequence, a weakly decreasing sequence, or a weakly increasing then weakly decreasing sequence. This order restriction must be true regardless of the shape of the genealogy at the QTL. The NLR statistic is not a very good approximation to the BF, in particular because it can never be negative. As far as I know, there is no theoretical reason to believe that it should have good properties as a test statistic. However, as figures 2 and 3 show, tests based on the NLR are superior to tests based on $p_{\min} \times L$ and are not clearly distinguishable from tests based on the BF. For the simulated datasets studied here, once the lookup table of emission probabilities (11) has been computed, computing the NLR is over 10^4 times faster than computing the BF. Furthermore, a Viterbi-like algorithm (see Durbin *et al.* 1998) for computing the NLR has time complexity $O(L \times n_d)$, compared with the CPQ algorithm for computing the BF which has time complexity $O((L + d_\mu) \times n_d^2)$.

It may concern some readers that the critical regions and sizes and powers of tests were all estimated while allowing the numbers of cases, controls and marker SNPs all to vary across simulations. To interpret results acquired in this way, a formal classical framework would require us to view the genotype relative risk g as the single parameter, and the number of case chromosomes n_d and number of SNPs L as random variables. It is true that even in such a framework we would normally wish to perform tests conditional on the values of ancilliary variables such as n_d and L that contain no information about whether there is a QTL in the region. However, it is a feature (or weakness) of classical inference that one is often free to choose whether to condition on any given variable (but see e.g. Jaynes 1976, Robinson 1979). The present results therefore do have a sound classical interpretation. In any case, the small number of simulations performed here do not allow the luxury of estimating critical regions conditional on n_d or L . The simulation procedure as used reflects a likely feature of real datasets, that SNP density will be higher in regions of the genome where the genealogy is deeper. To alter the simulation procedure so that all simulated datasets had the same value

of L would require the introduction of an *ad hoc* algorithm to select the L markers to be used from a larger number of candidates.

As shown in figure 4, the null distributions of both test statistics show a negative relationship with L . The negative relationship is most pronounced for the $2 \ln \text{BF}$ statistic, for the situation where there are errors in allele frequency estimation. In this case a linear regression of $2 \ln \text{BF}$ on L had a slope significantly different from zero ($p = 0.010$), and if the values of $2 \ln \text{BF}$ are partitioned into two groups according to the rank of L , the hypothesis that they are drawn from the same distribution can be rejected using a Kolmogorov–Smirnov test ($p = 0.004$). These tests do not detect significant dependence ($p > 0.05$) for the $2 \ln \text{BF}$ statistic when the allele frequencies are known exactly, or for the $p_{\min} \times L$ statistic.

Although the simulations described here are adequate for demonstrating the superiority of the BF based test over the p_{\min} based test, we should be cautious about extrapolating from the current results. In particular, it seems that the arbitrary ($2 \ln \text{BF} > 2 \ln(\frac{1-\alpha}{\alpha})$) or approximate (Bonferonni) critical regions described above will become more conservative as SNP number or density increases. Performing tests that are not conditioned on SNP number and density will introduce recognisable subset biases (see e.g. Robinson 1979). In a real situation, a critical region should be determined using simulations conditioned on as many ancillary statistics of the observed data as possible, although for complex simulation models it may be a matter of guesswork which statistics are approximately ancillary. An approach that could be most useful in practice is a variant of the permutation test of Churchill and Doerge (1994). This could be applied if there were matched pairs of pools of cases and controls, and each pair were typed in separate DNA pooling experiments (Shiffman *et al.* 2004). Then the phenotype labels could be permuted within each pair, giving a set of equiprobable values for any test statistic under the null hypothesis. Such an approach could not be explored here because it would require too much computation.

5.2. Sensitivity to prior specification

It is important to appreciate that the Bayes factor does not depend on the prior probabilities for the two models (QTL or no QTL), but *does* depend on the priors for the parameters within the QTL model. Misspecification of these priors could adversely influence the performance of the BF as a test statistic, and it is important to examine typical levels of robustness to the prior. To explore this, I compare the analyses above that used relatively flat generic priors to analyses that used priors that were in a way optimised for the simulated datasets under consideration.

Note that the prior for μ is correct, but that the approximate model here uses two other parameters τ and ρ that do not have any direct correspondance to parameters of the coalescent model that the data were simulated under. It is therefore difficult to say what the best prior is for analysing the simulated datasets. Loosely speaking, we might imagine that for any one simulated dataset, in the limit of an infinite amount of informative data the posterior for τ or ρ would converge to a single value, which we could call the “best approximating” value for that dataset. However, with less than an infinite amount of data the posterior mean for either variable would lie somewhere between the prior mean and the best approximating value. Thus the distribution of posterior means across simulations would be (very loosely speaking) inbetween the degenerate distribution at the prior mean, and the distribution of best approximating values. Figure 5 shows that this is indeed the case for μ , for which the prior mean is 0.5 and the true correct prior is uniform on $[0, 1]$. The distributions of posterior means for τ and ρ shown in figure 5 suggests a lognormal prior for τ (with $\ln(\tau)$ having prior mean 6.8 and prior standard deviation 0.74) and a beta prior for ρ (with $R_1 = 3.2$ and $R_0 = 7.8$, ρ having prior mean 0.29). Here I am assuming independent priors. Note that this exercise in prior specification was totally *ad hoc*.

As can be seen in figures 2 and 3, the ROC of the test statistic $2 \ln \text{BF}$ computed using these priors is hardly different better than that using the original priors. The power for tests of sizes $\alpha = 0.05$ and $\alpha = 0.01$ is not significantly different, based on 500 simulations. This suggests that the performance of the BF as a test statistic, for these datasets, is quite robust to prior specification within the QTL model.

Because most of the computation in QPQ can be reused, computing the BF for a different prior took on average less than three minutes, compared with the 36 minutes required to compute the BF for the original prior.

5.3. Estimation of QTL Position

Figures 6 and 7 show analyses of four randomly chosen simulated datasets with QTLs ($g = 4$). These illustrate the fact that these datasets contain only weak information about the position of the QTL (or at least that the Bayesian method described here only extracts weak information). It nonetheless seems worthwhile to examine how much information is present.

It has been suggested that the map position of the marker with the most significant single point test result (i.e. the minimum p -value) would be a “good” point estimate for the position of the QTL (Kaplan and Morris 2001a,b). However, I point out that it is asymptotically

inadmissible for a model very similar to the one assumed here. This argument considers the limit of a QTL of small effect. One can imagine models where the position of the marker with the minimum p -value, $\hat{\mu}_{\min p}$, will tend to become uniformly distributed on $(0, 1)$, independent of the true value of μ , as the effect of the QTL tends to zero. The estimator $\hat{\mu}_{\min p}$ then has expected loss $\mu(1 - \mu) + \frac{1}{2}$ under absolute error loss and $\frac{1}{3} - \mu(1 - \mu)$ under squared error loss. The estimator $\hat{\mu} = \frac{1}{2}$ has uniformly lower expected loss, $|\frac{1}{2} - \mu|$ under absolute error loss and $(\frac{1}{2} - \mu)^2$ under squared error loss. This argument does not technically apply for the model simulated here because SNPs (including the QTL) tend to be concentrated in regions where the genealogy is deepest, so even completely ignoring the genotype data, the position of any SNP is informative about the positions of all other SNPs including the QTL. It does however suggest that better point estimates may be found, and suggests what their asymptotic behaviour ought to be, at least approximately.

The performance of different methods for estimating the position of the QTL was assessed using the 500 simulations with $g = 4$, for the two situations with and without errors in allele frequency estimation. Due to the nature of the simulations performed here, the errors reported are averaged over the distribution of the true value of μ . They are therefore not classical expected losses in the strict sense, but expected losses averaged with respect to a distribution of parameter values. Bayesian point estimators have uniquely best performance when measured in this way (O’Hagan and Forster 2004 ch.5); the theory requires that the model and prior are both correct. In particular, under squared error losses the average expected loss is minimised by the posterior mean, and under absolute error losses the average expected loss is minimised by the posterior median. As shown in table 4, point estimators derived from the posterior calculated using the Bayesian method described here are superior to $\hat{\mu}_{\min p}$, the map location of the marker with the smallest p -value. When allele frequencies in each pool are known exactly the Bayesian analysis produces a 21% reduction in root average mean squared error and a 13% reduction in average mean absolute error. When there are errors in allele frequency estimation the figures are similar, 18% and 11% respectively. The nonparametric method developed previously by me (Johnson 2005) produces point estimates that are competitive with the Bayesian method under squared error losses.

Figures 8 and 9 show results from the 500 datasets simulated with $g = 4$. The coverage of credibility intervals constructed from the marginal posterior for μ falls well below nominal levels. This suggests strongly that the simple model used for the analyses is not a good approximation to the more realistic model the data were simulated under. One way to improve the model would be to allow a more realistic model for the shape of the genealogy at the QTL. To explicitly model this genealogy and hence the joint distribution of breakpoints between ancestral and nonancestral chromosome would require something like the MCMC sampler of Rannala and Reeve (2001) or Morris *et al.* (2002). Although taking such an

approach is highly desirable, it may not scale well to large datasets and it seems worthwhile to investigate approximations.

One approximation is the “pairwise correction” derived by McPeck and Strahs (1999) and justified by them by the use of a quasi-score function, and used in a Bayesian context by Morris *et al.* (2000). Essentially, this involves flattening the likelihood function by raising all likelihoods to a power $w_n = (1 + (n - 1)c_n)^{-1} < 1$. Here c_n is the pairwise correlation over sampled chromosomes of the conditional score function for the position of the QTL. An expression for c_n for a coalescent model is given in appendix D of McPeck and Strahs (1999). The n in this equation (which c_n also depends on) is the number of chromosomes carrying the QTL. It is not at all clear whether or how this correction should be applied in the present context, because (i) as noted by Morris *et al.* (2000) the quasi-score justification used by McPeck and Strahs (1999) does not apply in a Bayesian setting, (ii) in the present work the likelihood is never written as a conditional product across chromosomes carrying the QTL, (iii) it is not known how many chromosomes carry the QTL, and (iv) in my computational implementation no proper likelihoods are ever calculated, only likelihoods marginal to (π_1, \dots, π_L) . However, the following ad-hoc approach does produce corrected credibility intervals that achieve coverage very close to their nominal levels. The procedure is to first estimate n by $n_d E(\rho)$, the product of the number of case chromosomes and the posterior expectation of ρ , and then to flatten the marginal posterior for μ by raising it to a power w_n and renormalising. For the simulations performed here, w_n had median 0.56 and interquartile range 0.48–0.63. When this procedure was applied, good agreement between nominal and achieved coverage is obtained (figures 8 and 9). This suggests that the most serious misspecification of the current model is the assumption of a star shaped genealogy, rather than the assumption of linkage equilibrium in nonancestral blocks or the absence of the disease variant in the control pool.

5.4. Application to real data

It is not really possible to examine the effectiveness of the Bayesian method described here on real data, due to a lack of relevant published datasets. Primarily for the purpose of comparison with other fine scale mapping methods, I have applied it to the dataset of Hosking *et al.* (2002), and to quasi-synthetic datasets generated from that dataset. Hosking *et al.* (2002) collected data using individual genotyping. In order to pretend that the data were acquired using DNA pooling, I use a hypergeometric error model to relate the observed counts with missing data to the underlying full data that were not observed. This assumes the data are missing at random within and across SNPs.

To my knowledge, no fine scale mapping method has been published that does not perform well on the data of Hosking *et al.* (2002). Therefore, observing that the present method performs acceptably, as shown in figure 10, is not necessarily encouraging. To simulate a disease with a complex genetic basis, I generated three datasets by randomly relabelling controls as cases with probability 10%, 20% or 30%. As shown in figure 10, on all four datasets 95% credibility intervals covered the true location of the CYP2D6 gene after the correction factor of (McPeck and Strahs 1999) had been applied to flatten the posterior. This provides weak evidence that the method developed here may be reliable for mapping QTLs from real data.

6. Discussion

In this paper I have described and tested a Bayesian method for detecting and mapping a QTL, using multilocus data collected using DNA pooling within two trait groups.

Relatively recently, likelihood based fine scale mapping methods have been developed for genotype data that build on previous haplotype based analyses by treating the unobserved haplotypes as missing data and integrating over all possible haplotypes that are consistent with the observed genotypes. This integration can be performed either using Markov chain Monte Carlo (MCMC) (Liu *et al.* 2001, Reeve and Rannala 2002, Morris *et al.* 2003) or using exact numerical methods for hidden Markov models (Zhang and Zhao 2002). Data from DNA pools are estimated counts of alleles at each locus with no phase information. Fine scale mapping from genotype data and from DNA pools can in theory be regarded as closely related missing data problems.

The approach taken in this paper combines elements of the approaches of Zhang and Zhao (2002) and of Morris *et al.* (2000) and Liu *et al.* (2001). Like Zhang and Zhao (2002), I use a model that is sufficiently simple that I can use hidden Markov model (HMM) methods to sum over all possible haplotypes that are consistent with the observed data. However, after computing the likelihood using a propagation algorithm, Zhang and Zhao (2002) then maximise that likelihood with respect to the remaining model parameters. In contrast and like Morris *et al.* (2000) and Liu *et al.* (2001), I embed the HMM within a fully Bayesian approach and compute posterior probability distributions for the quantities of interest.

One advantage of a Bayesian approach is that probability statements can be made directly about quantities of interest. For example, we can state the probability that there is QTL in any given region, including the whole region under study. Thus, mapping and detecting a QTL are intimately related aspects of the same analysis. They are different infer-

ences that are made from the same posterior probability distribution. Within the Bayesian framework there is no need to choose between a bewildering array of estimators, test statistics and methods for correcting for multiple testing; the approach has a pleasing simplicity, at least conceptually.

However, the probabilities computed in a Bayesian analysis are only meaningful if the model and prior are realistic. The Catch-22 is that in order to compute Bayesian posterior probabilities, I had to assume a model that was worryingly oversimplified and not very believable. The present work is therefore best regarded as a step towards Bayesian analysis of data collected using DNA pooling. It may be helpful to draw parallels with methods for analysis of genotype data (collected using individual typing). Sadly, the present method allows us to make inferences assuming a model less elaborate than the one of Morris *et al.* (2000), whereas we might aspire to being able to assume a model like the one of Morris *et al.* (2002) or Zollner and Pritchard (2005). However, Bayesian analysis of such realistic models has required Markov chain Monte Carlo (MCMC) to integrate over high dimensional spaces of auxiliary variables or missing data. Such computationally intensive approaches may have difficulty handling large datasets. In contrast, the method described here is relatively fast, and large datasets could be analysed with realistic computational resources. For example, 27 processor-days would be required to analyse data from a whole genome scan with 100 cases, 500,000 SNPs, and evaluation of the posterior at points 50kb apart. In contrast, Zollner and Pritchard (2005) estimate that their MCMC based procedure for data from individual typings would take 85 processor-years for the same scale of analysis. A further advantage of avoiding Monte Carlo methods is that the large numbers of analyses needed for a sliding window analysis, or a permutation test, can be performed without needing human intervention to adjust mixing parameters or monitor convergence. Finally and perhaps most significantly, I am able to compute a Bayes factor (BF) to compare models in which there is, and is not, a disease QTL in the whole region of interest. To my knowledge, no association mapping method using genotype data is able to do this, although Patterson *et al.* (2004) are able to compute a BF for *admixture* mapping using genotype data.

There is a Bayesian justification for the present method. (“This is the best model for which a Bayesian analysis of data from DNA pools is currently possible.”) However, serious concerns about model inadequacy (“Well, that model simply isn’t good enough!”) mean that, in this paper, I have mostly focussed on the classical frequentist justification. Using simulations assuming a more realistic model, I have shown that the present method is uniformly superior to classical single point methods of analysis. Single point methods are the most obvious way to analyse data collected using DNA pooling, although composite likelihood methods (Terwilliger 1995, Xiong and Guo 1997, Collins and Morton 1998, Maniatis *et al.* 2004, 2005) could also be used. The simulation results demonstrate that the

BF computed using the present method makes a more powerful test for the presence of a QTL than the minimum p -value from single point tests, that the posterior density for the position of the QTL leads to a better point estimator than the position of the marker with the minimum p -value, and that well calibrated credibility intervals can be derived from the posterior density for the position of the QTL, after applying the correction of McPeck and Strahs (1999).

The performance of composite likelihood (CL) methods was not examined here. This was because no CL method has been developed that allows errors in allele frequency estimation, and because, to my knowledge, no CL method assumes a model that is obviously more realistic than the model assumed by the present method. In particular, all CL methods implicitly assume linkage equilibrium in non-ancestral blocks of chromosome. In the notation of the present paper, CL methods assume that the number of chromosomes carrying ancestral haplotype at the i -th SNP, x_i , is conditionally independent across SNPs. Even a poor model that does capture some aspect of the dependence across SNPs, such as the star shaped genealogy assumed here, seems preferable. To my knowledge, there is no CL method that produces well calibrated confidence or credibility intervals. Perhaps because of this, Maniatis *et al.* (2005) state that “[t]he main objective in positional cloning is to estimate the kb location of a causal SNP as accurately as possible, with its support interval an important but secondary objective.” However, it seems to me that we should focus on methods for computing well calibrated credibility intervals, and ideally a well calibrated posterior density. The acid test is to ask whether a statistical method informs us about what is a good action or decision to be taken subsequently. A point estimate for QTL position, without a reliable measure of precision, is not very helpful for planning future experiments to further refine the position of that QTL.

One of the more surprising results is that, in the simulations performed here, the non-parametric likelihood ratio (NLR) test derived from the method proposed previously by me (Johnson 2005) is basically as powerful as the BF for detecting a QTL. This is surprising because there is no theoretical basis for the NLR test statistic, but a strong theoretical basis for the BF test statistic. Since the NLR can be computed much more quickly, both in absolute and complexity terms, its performance in simulations over a wider range of parameters will be examined in a subsequent paper.

Given that the NLR performs as well as the BF for detecting a QTL, but that the BF is much more expensive to compute, one might reasonably ask what are the benefits of the Bayesian method described here. Firstly, the BF has a Bayesian interpretation, and since it can be negative it can indicate Bayesian sense evidence in favour of there being no QTL. The NLR test statistic can never be negative, has no direct Bayesian interpretation, and

is not a good approximation to the BF. Secondly, the posterior median from the Bayesian method provides superior point estimates under absolute error losses. Thirdly, the Bayesian method produces well calibrated credibility intervals, but the profile likelihood method I proposed previously does not (see figure 4 of Johnson 2005). Finally, the unconditional coverage frequencies of credibility intervals say nothing about the conditional or Bayesian sense performance of a method. For multistage QTL mapping experiments we should probably guide our choice of where to type further markers using the typically complex, heavy tailed and often multimodel posterior distributions computed using the Bayesian method described here, as exemplified in figure 7. If analysing data from a whole genome scan, I would recommend a multistage analysis that first uses the NLR statistic to identify regions of interest, and then to use the CPQ algorithm to compute Bayes factors and posterior distributions for QTL position within those regions.

Given the large number of simplifications made in specifying the model used here, one might wonder why the method works at all. The three most obviously inadequate approximations are the star shaped genealogy, the absence of the disease allele in the control pool, and the assumption of linkage equilibrium in non-ancestral blocks of chromosome. I will briefly discuss these inadequacies in turn.

Figures 8 and 9 show that credibility intervals only achieve prescribed coverage levels when a correction is made for the genealogy not in fact being star shaped. This suggests a serious inadequacy of the model. This is further supported by the observation of the very similar ROC curves in figures 2 and 3 for the theoretically optimal BF (assuming a star shaped genealogy), and the NLR statistic that has no theoretical basis (but allows any shape genealogy; Johnson 2005). Addressing this inadequacy is likely to lead to greater power to detect a QTL, and perhaps smaller credibility intervals of a given size. However, it will be hard to achieve without imposing a substantial computational burden. In particular, it may become difficult to compute the BF test statistic if MCMC is used to integrate over genealogies at the QTL.

Although it is conceptually straightforward to allow blocks of ancestral chromosome in the control pool, this would increase the number of hidden states at each SNP from $(n_d + 1)$ to $(n_d + 1)(n_c + 1)$. Since the propagation algorithm (section 3.3) requires time that is quadratic in the number of hidden states, the analysis would be intractable using the current approach. As an alternative, any number of separate pools could be treated as conditionally independent HMMs, but then we would have to integrate over the high dimensional space of allele frequencies and ancestral haplotypes using MCMC or importance sampling (see below).

It is possible that the current model adapts to fit there being blocks of ancestral chro-

mosome in the control pool, by appropriate adjustment of the allele frequency parameters. Ancestral blocks that are explicitly modelled in the disease pool would then represent additional blocks beyond what would be expected according to the adjusted allele frequency parameters. If this was so, the parameter ρ might be best interpreted as representing the rate of *excess* disease alleles in the disease pool.

Since only marginal observations are available, the assumption of linkage equilibrium may be relatively innocuous. Since there is virtually no information in the data about linkage disequilibrium, introducing parameters describing linkage disequilibrium into the model might have little effect on inferences about the quantities of interest. It is possible to retain the present framework where all the data are modelled as a single HMM, but to include pairwise linkage disequilibrium by allowing allelic state along each chromosome to be a first order Markov chain (see e.g. Liu *et al.* 2001, Morris *et al.* 2002). This will be quite computationally expensive, but could be examined in the future.

For the parameters chosen for the simulations performed here, the benefits of the present Bayesian method are somewhat modest. It remains unclear whether there would be larger benefits for other values of the simulation parameters, in particular more SNPs in the dataset, and/or larger benefits from a Bayesian analysis with a more realistic model. Clarification of both points awaits access to substantial computational resources. It is worth commenting that many of the variables in the present model also feature in more elaborate models, and therefore the present approach could be used to generate (for example) a joint importance sampling distribution for the ancestral haplotype, allele frequencies, and age and position of the QTL.

Even the simulated datasets studied here were generated under a model that lacks realism in several respects. For example, in simulating errors in allele frequency estimation I have ignored differential amplification of the two alleles, which may cause estimates of allele frequencies obtained using DNA pools to be biased. This manifests itself as only a second order effect on the difference in allele frequency between case and control pools (Visscher and Le Hellard 2003). Differential amplification can be accommodated easily in the present method of analysis, for example by making $\hat{y}_{d,i}$ a vector consisting of data from the pool and also from heterozygous individuals or pools of known composition. Even if no data from heterozygotes is available, it is possible to compute a $\Pr(\hat{y}|y)$ by integrating over a distribution of differential amplification constants, like in the approach of Moskvina *et al.* (2005).

One feature of the posteriors calculated using the present method (and especially after McPeck and Strahs (1999) flattening) is that they are very heavy tailed, and so large credibility intervals (99%, 99.9%) tend to be very wide, perhaps almost as wide as credibility

intervals computed from the prior! This suggests that, if a series of fine scale mapping experiments were conducted using DNA pooling, we would not be making radical reductions in the size of the region under study at each stage, but rather would be increasing the density of markers in some regions more than others after each stage of analysis.

Software

A software package implementing the methods described here is available from the web site <http://homepages.ed.ac.uk/tobyj/software/> . Source code is available and the package can be distributed freely under the terms of the GNU general public licence (Free Software Foundation 1991).

REFERENCES

- Arnheim, N., C. Strange and H. Erlich (1985) Use of pooled DNA samples to detect linkage disequilibrium of polymorphic restriction fragments and human disease: Studies of the HLA class II loci. *Proc. Natl. Acad. Sci. USA* **82**:6970–6974.
- Bader, J. S., A. Bansal and P. Sham (2001) Efficient SNP-based tests of association for quantitative phenotypes using pooled DNA. *GeneScreen* **1**:143–150.
- Barcellos, L. F., W. Klitz, L. L. Field, R. Tobias, A. M. Bowcock, R. Wilson, M. P. Nelson, J. Nagatomi and G. Thomson (1997) Association mapping of disease loci, by use of a pooled DNA genomic screen. *Am. J. Hum. Genet.* **61**:734–747.
- Carlson, C. S., M. A. Eberle, M. J. Rieder, J. D. Smith, L. Kruglyak and D. A. Nickerson (2003) Additional SNPs and linkage-disequilibrium analyses are necessary for whole-genome association studies in humans. *Nature Genetics* **33**:518–521. doi:10.1038/ng1128.
- Churchill, G. A. and R. W. Doerge (1994) Empirical threshold values for quantitative trait mapping. *Genetics* **138**:963–971.
- Clayton, D. (2001) Population association. In *Handbook of Statistical Genetics*, edited by D. J. Balding, M. Bishop and C. Cannings, pp. 519–540. Wiley, Chichester, England.
- Collins, A. and N. E. Morton (1998) Mapping a disease locus by allelic association. *Proc. Natl. Acad. Sci. USA* **95**:1741–1745.

- Darvasi, A. and M. Soller (1994) Selective dna pooling for determination of linkage between a molecular marker and a quantitative trait locus. *Genetics* **138**:1365–1373.
- Durbin, R., S. R. Eddy, A. Krogh and G. Mitchison (1998) *Biological Sequence Analysis: Probabilistic Models of Proteins and Nucleic Acids*. Cambridge University Press, Cambridge.
- Free Software Foundation (1991) GNU general public license. Available from [<http://www.gnu.org/licenses/gpl.html>](http://www.gnu.org/licenses/gpl.html).
- Germer, S., M. J. Holland and R. Higuchi (2000) High-throughput SNP allele-frequency determination in pooled DNA samples by kinetic PCR. *Genome Research* **10**:258–266.
- Gilks, W. R., S. Richardson and D. J. Spiegelhalter (editors) (1996) *Markov Chain Monte Carlo in Practice*. Chapman and Hall, London.
- Hosking, L. K., P. R. Boyd, C. F. Xu, M. Nisum, K. Cantone, I. J. Purvis, R. Khakhar, M. R. Barnes, U. Liberwirth, K. Hagen-Mann, M. G. Ehm and J. H. Riley (2002) Linkage disequilibrium mapping identifies a 390 Kb region associated with CYP2D6 poor drug metabolising activity. *The Pharmacogenomics Journal* **2**:165–175. doi:10.1038/sj.tpj.6500096.
- Hudson, R. R. (2002) Generating samples under a Wright–Fisher neutral model of genetic variation. *Bioinformatics* **18**:337–338.
- Jaynes, E. T. (1976) Confidence intervals vs. Bayesian intervals. In *Foundations of Probability Theory, Statistical Inference, and Statistical Theories of Science*, edited by W. L. Harper and C. A. Hooker, volume 2, pp. 175–257. D. Reidel, Dordrecht.
- Johnson, T. (2005) Multipoint linkage disequilibrium mapping using multilocus allele frequency data. *Annals of Human Genetics* **69**:474–498. doi:10.1046/j.1529-8817.2005.00178.x.
- Kaplan, N. and R. Morris (2001a) Issues concerning association studies for fine mapping a susceptibility gene for a complex disease. *Genetic Epidemiology* **20**:432–457.
- Kaplan, N. and R. Morris (2001b) Prospects for association-based fine mapping of a susceptibility gene for a complex disease. *Theoretical Population Biology* **60**:181–191. doi:10.1006/tpbi.2001.1537.
- Kruglyak, L. (1999) Prospects for whole-genome linkage disequilibrium mapping of common disease genes. *Nature Genetics* **22**:139–144.

- Lander, E. S. (1996) The new genomics: Global views of biology. *Science* **274**:536–539.
- Le Hellard, S., S. J. Ballereau, P. M. Visscher, H. S. Torrance, J. Pinson, S. W. Morris, M. L. Thomson, C. A. M. Semple, W. J. Muir, D. H. R. Blackwood, D. J. Porteous and K. L. Evans (2002) SNP genotyping on pooled DNAs: Comparison of genotyping technologies and a semi automated method for data storage and analysis. *Nucleic Acids Research* **30**:e74.
- Li, N. and M. Stephens (2003) Modeling linkage disequilibrium and identifying recombination hotspots using single-nucleotide polymorphism data. *Genetics* **165**:2213–2233.
- Liu, J. S. (2001) *Monte Carlo Strategies in Scientific Computing*. Springer–Verlag, New York.
- Liu, J. S., C. Sabatti, J. Teng, B. J. Keats and N. Risch (2001) Bayesian analysis of haplotypes for linkage disequilibrium mapping. *Genome Research* **11**:1716–1724. doi:10.1101/gr.194801.
- Maniatis, N., A. Collins, J. Gibson, W. Zhang, W. Tapper, and N. E. Morton (2004) Positional cloning by linkage disequilibrium. *Am. J. Hum. Genet.* **74**:846–855.
- Maniatis, N., N. E. Morton, J. Gibson, C.-F. Xu, L. K. Hosking and A. Collins (2005) The optimal measure of linkage disequilibrium reduces error in association mapping of affection status. *Human Molecular Genetics* **14**:145–153. doi:10.1093/hmg/ddi019.
- McPeck, M. S. and A. Strahs (1999) Assessment of linkage disequilibrium by the decay of haplotype sharing, with application to fine-scale genetic mapping. *Am. J. Hum. Genet.* **65**:858–875.
- Morris, A. P., J. C. Whittaker and D. J. Balding (2000) Bayesian fine-scale mapping of disease loci, by hidden Markov models. *Am. J. Hum. Genet.* **67**:155–169.
- Morris, A. P., J. C. Whittaker and D. J. Balding (2002) Fine-scale mapping of disease loci via shattered coalescent modeling of genealogies. *Am. J. Hum. Genet.* **70**:686–707.
- Morris, A. P., J. C. Whittaker, C.-F. Xu, L. K. Hosking and D. J. Balding (2003) Multi-point linkage-disequilibrium mapping narrows location interval and identifies mutation. *Proc. Natl. Acad. Sci. USA* **100**:13442–13446. doi:10.1073/pnas.223503110.
- Moskvina, V., N. Norton, N. Williams, P. Holmans, M. Owen and M. O’Donovan (2005) Streamlined analysis of pooled genotype data in SNP-based association studies. *Genetic Epidemiology* **28**:273–282. doi:10.1002/gepi.20062.

- Mott, R., C. J. Talbot, M. G. Turri, A. C. Collins and J. Flint (2000) A method for fine mapping quantitative trait loci in outbred animal stocks. *Proc. Natl. Acad. Sci. USA* **97**:12649–12654.
- Norton, N., N. M. Williams, M. C. O’Donovan and M. J. Owen (2004) DNA pooling as a tool for large-scale association studies in complex traits. *Annals of Medicine* **36**:146–152. doi:10.1080/07853890310021724.
- O’Hagan, A. and J. Forster (2004) *Bayesian Inference*, volume 2B of *Kendall’s Advanced Theory of Statistics*. Arnold, London, 2nd edition.
- Patterson, N., N. Hattangadi, B. Lane, K. E. Lohmueller, D. A. Hafler, J. R. Oksenberg, S. L. Hauser, M. W. Smith, S. J. O’Brien, D. Altshuler, M. J. Daly and D. Reich (2004) Methods for high-density admixture mapping of disease genes. *Am. J. Hum. Genet.* **74**:979–1000.
- Rannala, B. and J. P. Reeve (2001) High-resolution multipoint linkage-disequilibrium mapping in the context of a human genome sequence. *Am. J. Hum. Genet.* **69**:159–178.
- Reeve, J. P. and B. Rannala (2002) DMLE+: Bayesian linkage disequilibrium mapping. *Bioinformatics* **18**:894–895.
- Risch, N. and K. Merikangas (1996) The future of genetic studies of complex human diseases. *Science* **273**:1516–1517.
- Risch, N. and J. Teng (1998) The relative power of family-based and case-control designs for linkage disequilibrium studies of complex human diseases. I. DNA pooling. *Genome Research* **8**:1273–1288.
- Risch, N. J. (2000) Searching for genetic determinants in the new millennium. *Nature* **405**:847–856.
- Robinson, G. K. (1979) Conditional properties of statistical procedures. *The Annals of Statistics* **7**:742–755.
- Sham, P., J. S. Bader, I. Craig, M. O’Donovan and M. Owen (2002) DNA pooling: A tool for large-scale association studies. *Nature Reviews Genetics* **3**:862–871. doi:10.1038/nrg930.
- Shiffman, D., M. M. Luke, O. A. Iakoubova, C. R. Pullinger, B. E. Aouizerat, C. A. Zellner, T. A. Ports, A. D. Michaels, D. W. Drew, J. J. Catanese, D. U. Leong, D. M. Liu, J. Z. Louie, D. Lew, C. H. Tong, D. A. Ross, L. B. McAllister, C. M. Rowland,

- K. F. Lau, J. J. Devlin, M. J. Malloy and J. P. Kane (2004) Novel genetic markers associated with myocardial infarction: A genomic scale scan of putative functional polymorphisms. Poster from American College of Cardiology meeting. Available from <http://www.celeradiagnostics.com/cdx/publications>.
- Silverman, B. W. (1986) *Density Estimation*. Chapman and Hall, London.
- Terwilliger, J. (1995) A powerful likelihood method for the analysis of linkage disequilibrium between trait loci and one or more polymorphic marker loci. *Am. J. Hum. Genet.* **56**:777–787.
- Visscher, P. M. and S. Le Hellard (2003) Simple method to analyze SNP-based association studies using DNA pools. *Genetic Epidemiology* **24**:291–296. doi:10.1002/gepi.10240.
- Xiong, M. and S.-W. Guo (1997) Fine-scale genetic mapping based on linkage disequilibrium: Theory and applications. *Am. J. Hum. Genet.* **60**:1513–1531.
- Zhang, S. and H. Zhao (2000) Linkage disequilibrium mapping in populations of variable size using the decay of haplotype sharing and a stepwise-mutation model. *Genetic Epidemiology* **9**(Suppl 1):S99–S105.
- Zhang, S. and H. Zhao (2002) Linkage disequilibrium mapping with genotype data. *Genetic Epidemiology* **22**:66–77.
- Zollner, S. and J. K. Pritchard (2005) Coalescent-based association mapping and fine mapping of complex trait loci. *Genetics* **169**:1071–1092. doi:10.1534/genetics.104.031799.

Table 1. Frequently used notations.

Symbol	Meaning
a_i	Allele present (0 or 1) on ancestral haplotype at i -th SNP
b, b'	Backwards variables, see (13) and (14)
$B(\alpha, \beta)$	Beta distribution with parameters α and β
$\text{Bin}(n, p)$	Binomial distribution with parameters n and p
$\text{Bin}(x, n, p)$	Probability of drawing x from a binomial distribution with parameters n and p
BF	Bayes factor
CPQ	Cartesian product quadrature
d_μ	Number of design points used for μ in quadrature algorithm
e_i	Precision of assay used to genotype i -th SNP
$E(\lambda)$	Exponential distribution with rate parameter λ (mean $1/\lambda$)
g	Genotype relative risk; factor by which disease allele increases penetrance or risk
$G(\alpha, \beta)$	Gamma distribution with shape parameter α and scale parameter β
HMM	Hidden Markov model
i	Index of SNP, $i = 1, \dots, L$
i.b.d.	Identical by descent
L	Number of SNPs
m_i	Map position of the i -th marker
MCMC	Markov chain Monte Carlo
n_c, n_d	Number of chromosomes in control and case pools respectively
$N(\mu, \sigma^2)$	Normal distribution with mean μ and variance σ^2
NLR	Nonparametric likelihood ratio, see (30)
p_{\min}	Smallest p -values out of L tests in single point analysis
$P_{i,a}$	Prior parameter: $\pi_i(a) \sim B(P_{i,a}, P_{i,1-a})$
r	Number of experimental replicates used to estimate $\Delta\hat{C}_t$
R	Prior parameter: $\rho \sim B(R_1, R_0)$
ROC	Receiver operating characteristics
T	Prior parameter: $\tau \sim E(T)$
x_i	Number of chromosomes in case pool carrying ancestral i.b.d. haplotype at i -th SNP
x_μ	Number of chromosomes in case pool carrying ancestral i.b.d. haplotype at position of QTL
$y_{c,i}(a)$	True count of allele a at i -th SNP in control pool
$y_{d,i}(a)$	True count of allele a at i -th SNP in case pool

Table 1—Continued

Symbol	Meaning
$\hat{y}_{c,i}(a)$	Estimated count of allele a at i -th SNP in control pool
$\hat{y}_{d,i}(a)$	Estimated count of allele a at i -th SNP in case pool
\hat{y}	Shorthand for $\hat{y}_{c,i}(1)$ or $\hat{y}_{d,i}(1)$ for some i
$\hat{\mathbf{y}}$	All the data
α	Nominal size (rate of type I error) of a test
$\Delta\hat{C}_t$	Estimated lag between PCR growth curves used to type DNA pool
γ_G	Penetrance (risk of disease) for genotype G at the QTL
μ	Map position of the disease locus
$\hat{\mu}_{\min p}$	Map position of SNP with smallest p -value in single point analysis
$\pi_i(1)$	Expected frequency of allele 1 at i -th SNP in non-ancestral chromosome
ρ	Expected frequency of disease allele in case pool
σ	Standard deviation of experimental error in estimation of $\Delta\hat{C}_t$
τ	Age of the disease allele

Table 2. Performance of tests to detect a disease QTL, when allele frequencies in each pool are known exactly.

Statistic	Method	Nominal size	Critical value	True size	Power
$2 \ln \text{BF}$	Arbitrary		0	0.080 (0.058, 0.107)	0.870 (0.837, 0.898)
$2 \ln \text{BF}$	Arbitrary	0.05 ^a	5.889	0.010 (0.003, 0.023)	0.710 (0.668, 0.749)
$p_{\min} \times L$	Bonferonni	0.05	0.05	0.040 (0.025, 0.061)	0.720 (0.678, 0.759)
$2 \ln \text{BF}$	Simulation	0.05	0.903	0.050 (0.033, 0.073)	0.842 (0.807, 0.873)
$p_{\min} \times L$	Simulation	0.05	0.063	0.050 (0.033, 0.073)	0.740 (0.699, 0.778)
$2 \ln \text{BF}$	Arbitrary	0.01 ^a	9.19	0.002 (0.000, 0.011)	0.628 (0.584, 0.67)
$p_{\min} \times L$	Bonferonni	0.01	0.010	0.000 (0.000, 0.006)	0.582 (0.537, 0.626)
$2 \ln \text{BF}$	Simulation	0.01	5.864	0.010 (0.003, 0.023)	0.710 (0.668, 0.749)
$p_{\min} \times L$	Simulation	0.01	0.027	0.010 (0.003, 0.023)	0.664 (0.621, 0.705)

^anot a nominal size in the classical sense but a nominal upper bound on the Bayesian sense error rate

Table 3. Performance of tests to detect a disease QTL, when there are errors in allele frequency estimation with $r = 2$ replicates and $\sigma = 0.2$ PCR cycles.

Statistic	Method	Nominal size	Critical value	True size	Power
$2 \ln \text{BF}$	Arbitrary		0	0.080 (0.058, 0.107)	0.782 (0.743, 0.817)
$2 \ln \text{BF}$	Arbitrary	0.05 ^a	5.889	0.008 (0.002, 0.020)	0.532 (0.487, 0.576)
$p_{\min} \times L$	Bonferonni	0.05	0.05	0.040 (0.025, 0.061)	0.560 (0.515, 0.604)
$2 \ln \text{BF}$	Simulation	0.05	0.723	0.050 (0.033, 0.073)	0.746 (0.705, 0.784)
$p_{\min} \times L$	Simulation	0.05	0.085	0.050 (0.033, 0.073)	0.642 (0.598, 0.684)
$2 \ln \text{BF}$	Arbitrary	0.01 ^a	9.19	0.000 (0.000, 0.006)	0.424 (0.380, 0.469)
$p_{\min} \times L$	Bonferonni	0.01	0.01	0.010 (0.003, 0.023)	0.432 (0.388, 0.477)
$2 \ln \text{BF}$	Simulation	0.01	4.28	0.010 (0.003, 0.023)	0.596 (0.552, 0.639)
$p_{\min} \times L$	Simulation	0.01	0.01	0.010 (0.003, 0.023)	0.432 (0.388, 0.477)

^anot a nominal size in the classical sense but a nominal upper bound on the Bayesian sense error rate

Table 4. Performance of point estimators of QTL position.

Estimator	Average expected loss under	
	squared error losses	absolute error losses
Allele frequencies known exactly		
$\hat{\mu}_{\min p}$	0.208 ²	0.120
Mean ($\mu \hat{\mathbf{y}}$)	0.165 ²	0.107
Median ($\mu \hat{\mathbf{y}}$)	0.166 ²	0.105
NP method	0.165 ²	0.112
Errors in allele frequency estimation		
$\hat{\mu}_{\min p}$	0.239 ²	0.146
Mean ($\mu \hat{\mathbf{y}}$)	0.195 ²	0.132
Median ($\mu \hat{\mathbf{y}}$)	0.203 ²	0.130
NP method	0.198 ²	0.136

List of Figures

- 1 Hierarchical or Bayesian network structure of the model. The region inside the rectangle is duplicated for each of L SNPs. Lines indicate the dependence structure of the model: Variables not connected are independent, conditional on all other variables in the model. 40
- 2 Sensitivity vs. specificity for $2 \ln \text{BF}$ (solid line) and $p_{\min} \times L$ (dashed line), when allele frequencies in each pool are known exactly. The dotted line shows the performance of $2 \ln \text{BF}$ computed using the priors obtained from figure 5, and the dot-dashed line shows the performance of a nonparametric likelihood ratio test statistic (Johnson 2005; see text). 41
- 3 Sensitivity vs. specificity for $2 \ln \text{BF}$ (solid line) and $p_{\min} \times L$ (dashed line), when there are errors in allele frequency estimation with $r = 2$ replicates and $\sigma = 0.2$ PCR cycles. The dotted line shows the performance of $2 \ln \text{BF}$ computed using the priors obtained from figure 5, and the dot-dashed line shows the performance of a nonparametric likelihood ratio test statistic (Johnson 2005; see text). 42
- 4 Sampling distribution of test statistics $2 \ln \text{BF}$ (top) and $p_{\min} \times L$ (bottom, on log scale) under null model ($g = 1$), as functions of L , the number of SNPs in the simulated data set. The 0.95 and 0.99 quantiles are shown as solid lines. The least squares linear regression is shown as a dotted line. Results shown are for the situation where there are errors in allele frequency estimation, but results are similar when allele frequencies are known exactly. 43
- 5 Original priors (dotted lines) and distribution of posterior expectations (solid lines) for the three parameters of the approximate model. This suggests more accurately specified priors (dashed lines) as described in the text. 44
- 6 Example simulated datasets with $g = 4$ and where allele frequencies are known exactly. Points are $-\log_{10} p$ for single point χ^2 tests. Dotted lines are posterior density and solid lines are posterior density with McPeck–Strahs correction. Vertical dashed lines show position of disease QTL. 45

7	The same simulated datasets as shown in figure 6, but with errors in allele frequency estimation with $\sigma = 0.2$ PCR cycles and $r = 2$ experimental replicates. Points are $-\log_{10} p$ for single point shrunk (Visscher and Le Hellard 2003) χ^2 tests. Dotted lines are posterior density and solid lines are posterior density with McPeck–Strahs correction. Vertical dashed lines show position of disease QTL.	46
8	Nominal and achieved coverage of credibility intervals for position of QTL, when allele frequencies are known exactly. Credibility intervals were constructed either without (dotted line) or with (solid line) the approximate correction factor of McPeck and Strahs (1999).	47
9	Nominal and achieved coverage of credibility intervals for position of QTL, when there are errors in allele frequency estimation, with $\sigma = 0.2$ and $r = 2$. Credibility intervals were constructed either without (dotted line) or with (solid line) the approximate correction factor of McPeck and Strahs (1999).	48
10	Analysis of data of Hosking <i>et al.</i> (2002; top panel), and quasi-synthetic datasets generated by randomly relabelling controls as cases with probability 10%, 20% or 30% (lower three panels, top to bottom). Points are $-\log_{10}(p)$ from single point χ^2 tests, and dashed and solid lines are the marginal posterior for disease gene position, without and with the correction factor of (McPeck and Strahs 1999). Vertical dashed lines show the true position of CYP2D6.	49

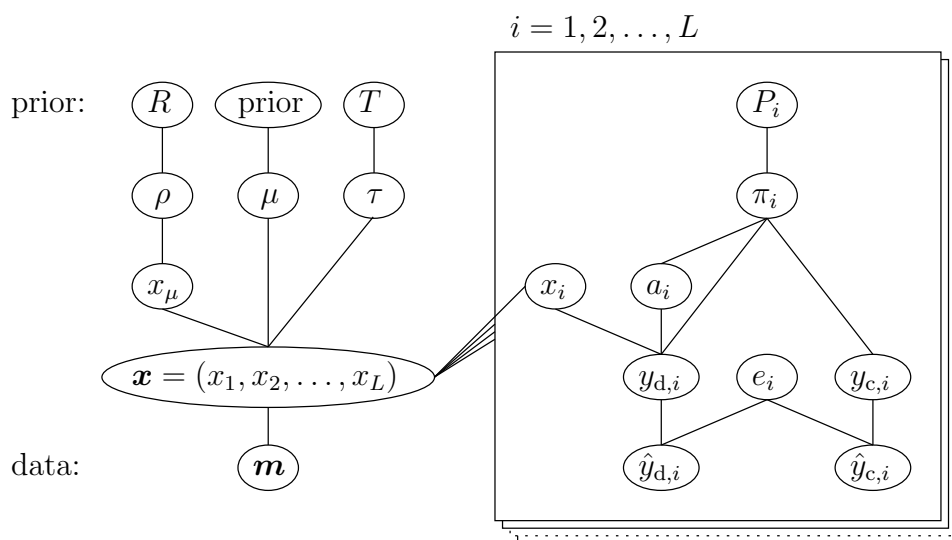


Fig. 1.— Hierarchical or Bayesian network structure of the model. The region inside the rectangle is duplicated for each of L SNPs. Lines indicate the dependence structure of the model: Variables not connected are independent, conditional on all other variables in the model.

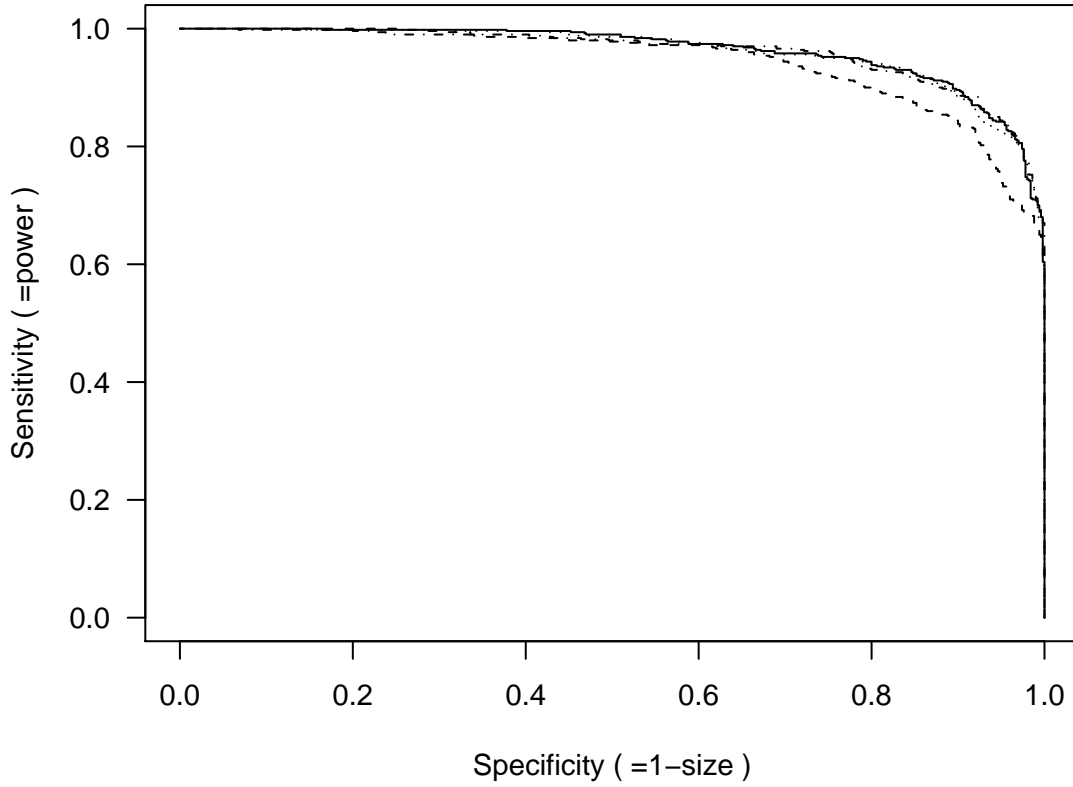


Fig. 2.— Sensitivity vs. specificity for $2 \ln \text{BF}$ (solid line) and $p_{\min} \times L$ (dashed line), when allele frequencies in each pool are known exactly. The dotted line shows the performance of $2 \ln \text{BF}$ computed using the priors obtained from figure 5, and the dot-dashed line shows the performance of a nonparametric likelihood ratio test statistic (Johnson 2005; see text).

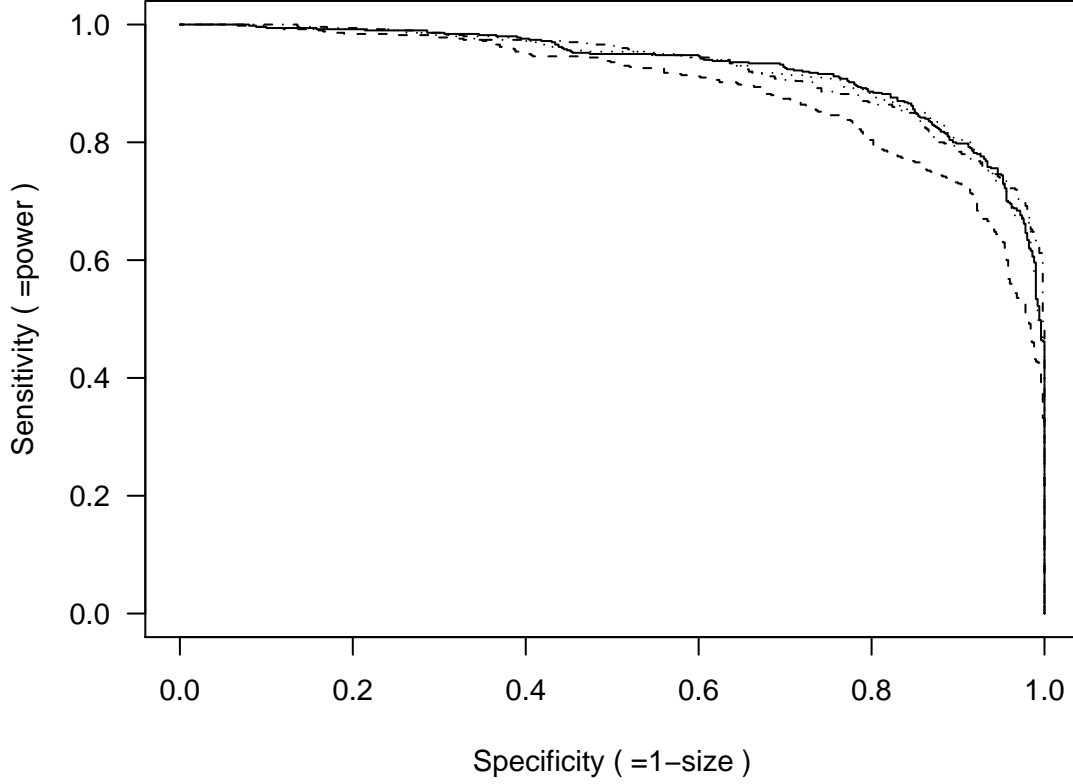


Fig. 3.— Sensitivity vs. specificity for $2 \ln \text{BF}$ (solid line) and $p_{\min} \times L$ (dashed line), when there are errors in allele frequency estimation with $r = 2$ replicates and $\sigma = 0.2$ PCR cycles. The dotted line shows the performance of $2 \ln \text{BF}$ computed using the priors obtained from figure 5, and the dot-dashed line shows the performance of a nonparametric likelihood ratio test statistic (Johnson 2005; see text).

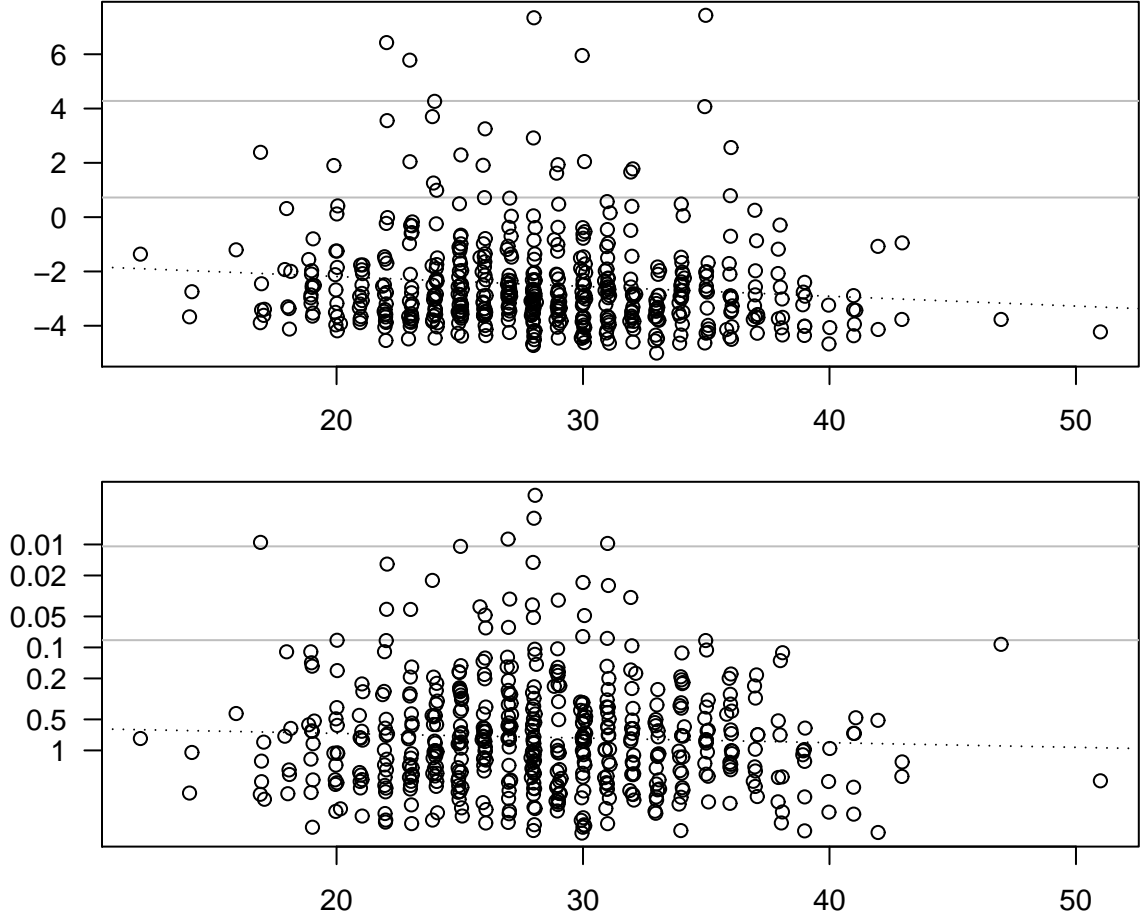


Fig. 4.— Sampling distribution of test statistics $2 \ln \text{BF}$ (top) and $p_{\min} \times L$ (bottom, on log scale) under null model ($g = 1$), as functions of L , the number of SNPs in the simulated data set. The 0.95 and 0.99 quantiles are shown as solid lines. The least squares linear regression is shown as a dotted line. Results shown are for the situation where there are errors in allele frequency estimation, but results are similar when allele frequencies are known exactly.

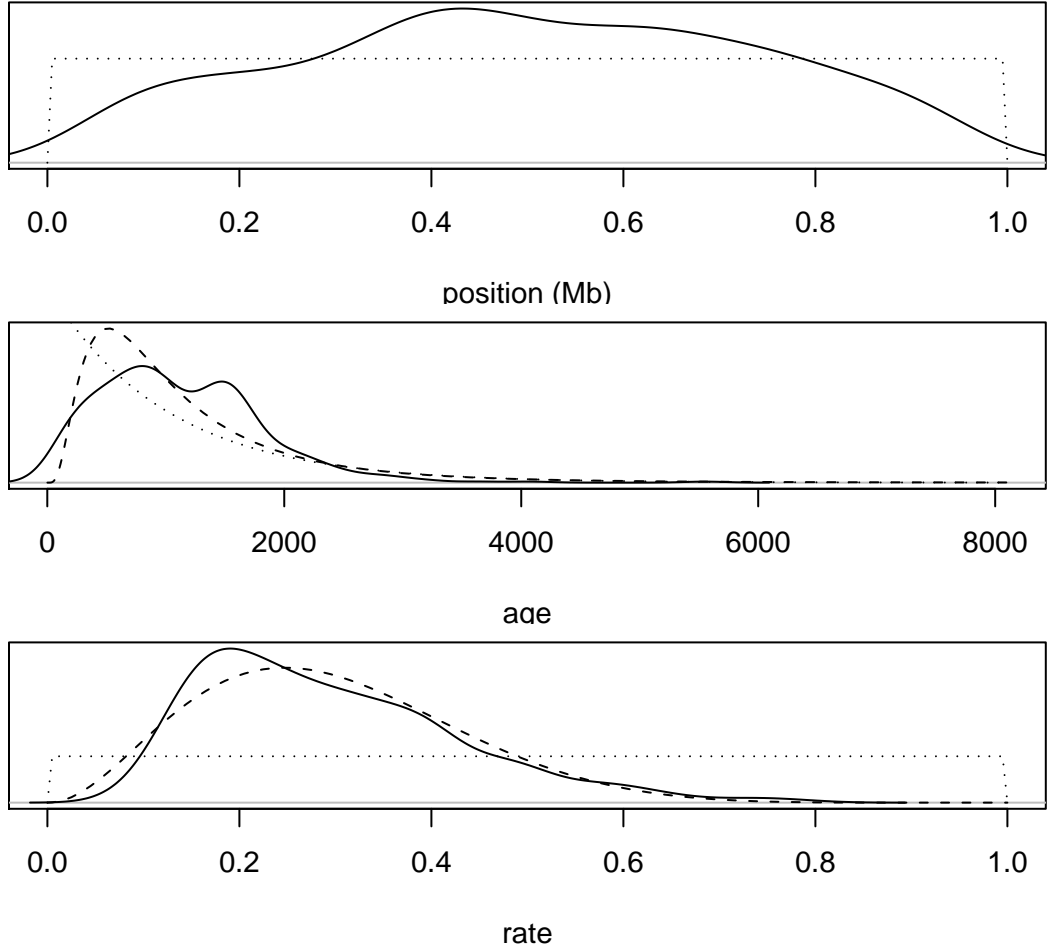


Fig. 5.— Original priors (dotted lines) and distribution of posterior expectations (solid lines) for the three parameters of the approximate model. This suggests more accurately specified priors (dashed lines) as described in the text.

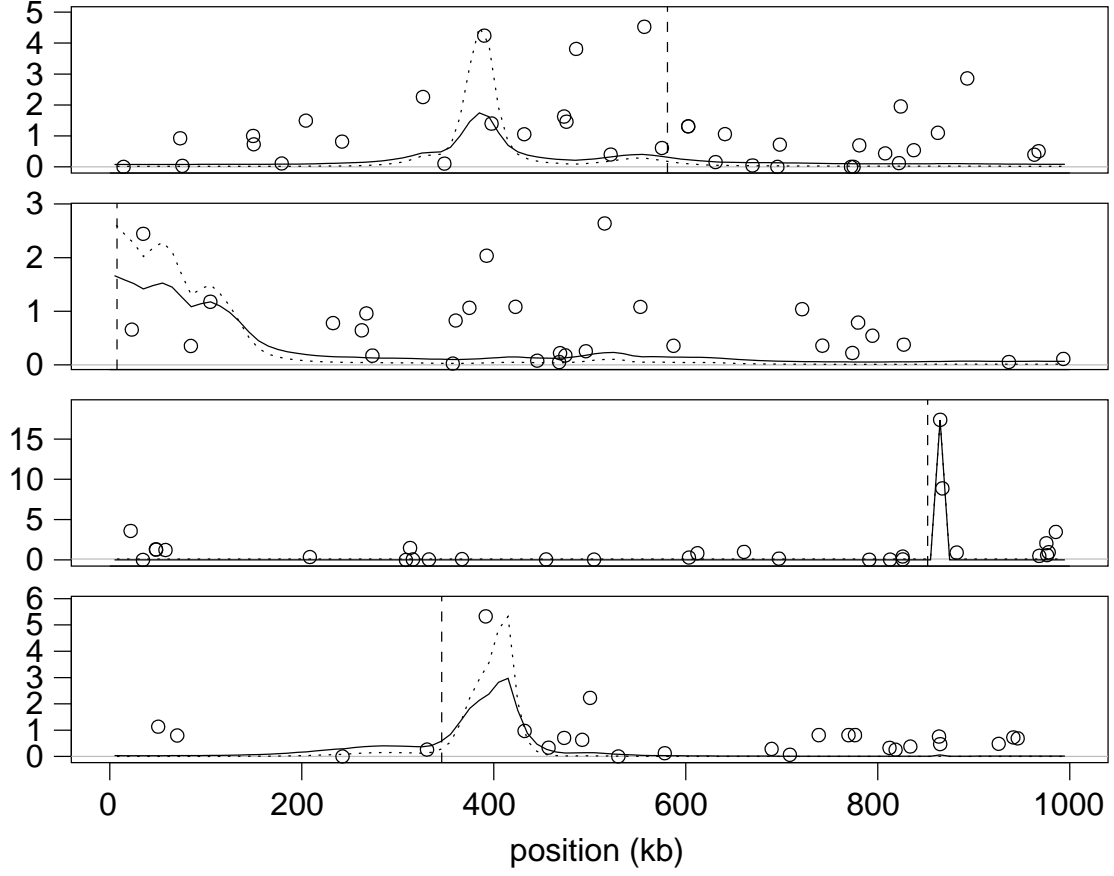


Fig. 6.— Example simulated datasets with $g = 4$ and where allele frequencies are known exactly. Points are $-\log_{10} p$ for single point χ^2 tests. Dotted lines are posterior density and solid lines are posterior density with McPeck–Strahs correction. Vertical dashed lines show position of disease QTL.

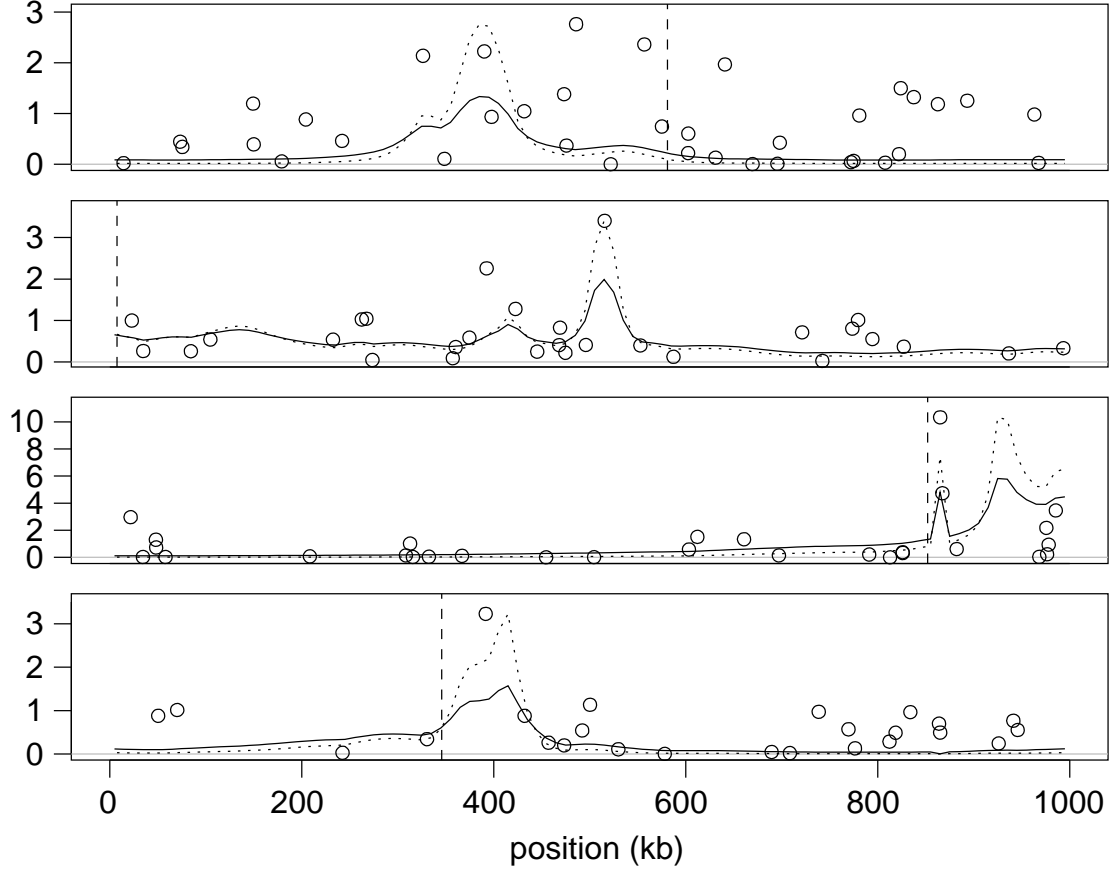


Fig. 7.— The same simulated datasets as shown in figure 6, but with errors in allele frequency estimation with $\sigma = 0.2$ PCR cycles and $r = 2$ experimental replicates. Points are $-\log_{10} p$ for single point shrunk (Visscher and Le Hellard 2003) χ^2 tests. Dotted lines are posterior density and solid lines are posterior density with McPeck-Strahs correction. Vertical dashed lines show position of disease QTL.

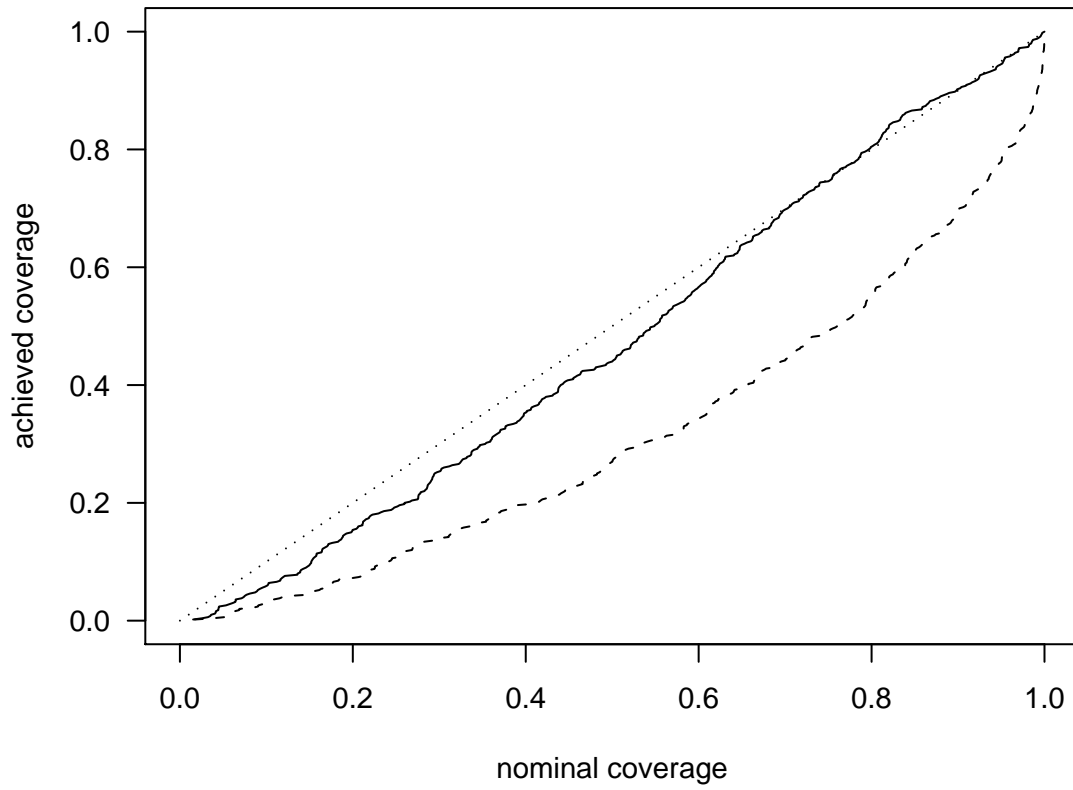


Fig. 8.— Nominal and achieved coverage of credibility intervals for position of QTL, when allele frequencies are known exactly. Credibility intervals were constructed either without (dotted line) or with (solid line) the approximate correction factor of McPeck and Strahs (1999).

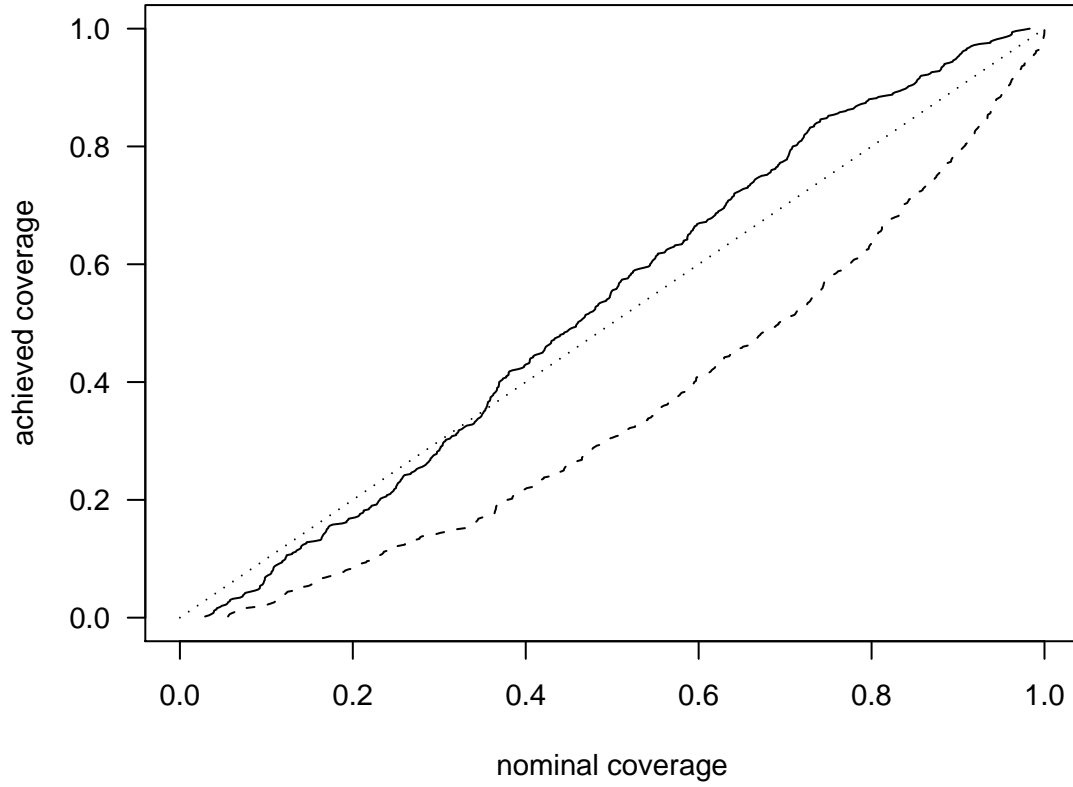


Fig. 9.— Nominal and achieved coverage of credibility intervals for position of QTL, when there are errors in allele frequency estimation, with $\sigma = 0.2$ and $r = 2$. Credibility intervals were constructed either without (dotted line) or with (solid line) the approximate correction factor of McPeck and Strahs (1999).

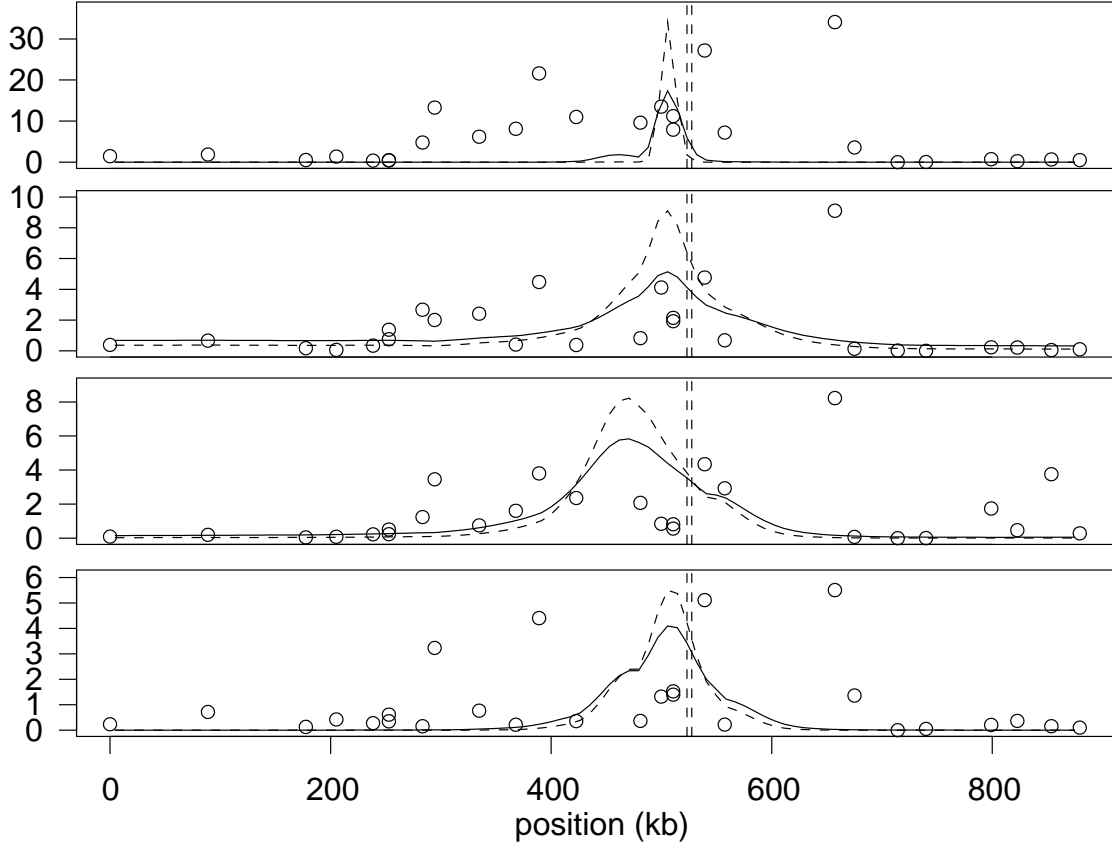


Fig. 10.— Analysis of data of Hosking *et al.* (2002; top panel), and quasi-synthetic datasets generated by randomly relabelling controls as cases with probability 10%, 20% or 30% (lower three panels, top to bottom). Points are $-\log_{10}(p)$ from single point χ^2 tests, and dashed and solid lines are the marginal posterior for disease gene position, without and with the correction factor of (McPeck and Strahs 1999). Vertical dashed lines show the true position of CYP2D6.